

THE DEMOCRATIC SOCIALIST REPUBLIC OF SRI LANKA
CEYLON ELECTRICITY BOARD

**FEASIBILITY STUDY
ON
UPPER KOTMALE
HYDROELECTRIC POWER DEVELOPMENT PROJECT**

**FINAL REPORT
VOLUME 2
APPENDIX I GEOLOGY**

AUGUST 1987

JAPAN INTERNATIONAL COOPERATION AGENCY



THE DEMOCRATIC SOCIALIST
REPUBLIC OF SRI LANKA

FEASIBILITY STUDY ON UPPER KOTMALE
HYDROELECTRIC POWER DEVELOPMENT PROJECT

FINAL REPORT
VOLUME 2
APPENDIX I

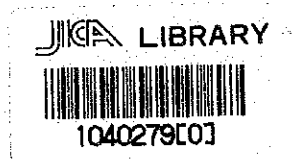
AUGUST 1

120
64.3
MPN

MPN
CR 9
87-122-2/4

THE DEMOCRATIC SOCIALIST REPUBLIC OF SRI LANKA
CEYLON ELECTRICITY BOARD

**FEASIBILITY STUDY
ON
UPPER KOTMALE
HYDROELECTRIC POWER DEVELOPMENT PROJECT**



FINAL REPORT

16884

VOLUME 2

APPENDIX I GEOLOGY

AUGUST 1987

JAPAN INTERNATIONAL COOPERATION AGENCY

国際協力事業団

| | | |
|-----------|-----------|-------------|
| 受入 月日 | '87.10.15 | 120 |
| 登録 No. | 16884 | 64.3 MPN |

APPENDIX I

GEOLOGY

APPENDIX I GEOLOGY

| | | <u>Page</u> |
|-----|-------------------------------------------------|-------------|
| I.1 | Topography and General Geology | I-6 |
| | I.1.1 General | I-6 |
| | I.1.2 Topography | I-6 |
| | I.1.3 General Geology | I-7 |
| I.2 | Investigations | I-9 |
| | I.2.1 General | I-9 |
| | I.2.2 Core Drilling | I-9 |
| | I.2.3 Seismic Prospecting Survey | I-13 |
| | I.2.4 Laboratory Testing | I-14 |
| I.3 | Geomorphological Study | I-15 |
| | I.3.1 Introduction | I-15 |
| | I.3.2 Ground Truth and Conclusions | I-17 |
| I.4 | Geology at Major Structure Sites | I-19 |
| | I.4.1 General | I-19 |
| | I.4.2 Caledonia Dam Site | I-23 |
| | I.4.3 Caledonia Dam Site Saddle | I-25 |
| | I.4.4 Talawakelle Dam Site | I-27 |
| | I.4.5 Caledonia Power Station | I-29 |
| | I.4.6 Talowakelle Power Station | I-31 |
| I.5 | Lugeon Test Results | I-36 |
| I.6 | Laboratory Test Results | I-42 |
| | I.6.1 General | I-42 |
| | I.6.2 Unconfined Compressive Strength | I-49 |
| | I.6.3 Triaxial Compressive Strength | I-51 |
| | I.6.4 Tensile Strength Test | I-52 |

| | <u>Page</u> |
|------------------------------------------------|-------------|
| I.6.5 Sonic Test | I-52 |
| I.6.6 Physical Test | I-54 |
| I.7 Site Evaluation | I-55 |
| I.7.1 Caledonia Dam Area | I-55 |
| I.7.2 Caledonia Dam Saddle Area | I-55 |
| I.7.3 Talawakelle Intake Dam Area | I-56 |
| I.7.4 Caledonia Power Station Area | I-56 |
| I.7.5 Talawakelle Power Station Area | I-57 |
| I.7.6 Tunnel Routes | I-58 |

List of Illustrations

| | | <u>Page</u> |
|------------|----------------------------------------------------------------------------------|-------------|
| FIG. I.1-1 | Restored Topo-map | I-F-1 |
| I.1-2 | Drainage Pattern | I-F-2 |
| I.1-3 | Relative Relief Map | I-F-3 |
| I.2-1 | Drilling Site and Seismic Prospecting Line for Caledonia Dam Area | I-F-4 |
| I.2-2 | Drilling Site and Seismic Prospecting Line for Talawakelle Dam Area | I-F-5 |
| I.2-3 | Drilling Site and Seismic Prospecting Line for Caledonia P/S Area | I-F-6 |
| I.2-4 | Drilling Site and Seismic Prospecting Line for Talawakelle P/S Area | I-F-7 |
| I.2-5 | Seismic Prospecting Line for Talawakelle P/S Upstream-alternative | I-F-8 |
| I.4-1 | Geological Route Map | I-F-9 |
| I.4-2 | Geological Structure Map | I-F-10 |
| | Legend for Geological Maps | I-F-11 |
| I.4-3 | Geological Map for Caledonia Dam Area | I-F-12 |
| I.4-4 | Geological Map for Caledonia Reservoir Area | I-F-13 |
| I.4-5 | Geological Map for Talawakelle Dam Area | I-F-14 |
| I.4-6 | Geological Map for Caledonia P/S Area | I-F-15 |
| I.4-7 | Geological Map for Talawakelle P/S Area | I-F-16 |
| | Legend for Geological Sections | I-F-17 |
| I.4-8 | Geological Section for Seismic Line SL: CD-1 | I-F-18 |
| I.4-9 | Geological Section for Seismic Line SL: CD-2 | I-F-19 |
| I.4-10 | Geological Section for Seismic Line SL: CD-3 | I-F-19 |
| I.4-11 | Geological Section for Seismic Line SL: CD-4 | I-F-20 |

| | <u>Page</u> |
|-----------------------------------------------------------------|-------------|
| I.4-12 Geological Section for Seismic Line SL: CD-5 | I-F-20 |
| I.4-13 Geological Section for Seismic Line SL: CD-6 | I-F-21 |
| I.4-14 Geological Section for Seismic Line SL: CD-7 | I-F-21 |
| I.4-15 Geological Section for Seismic Line SL: CD-8 | I-F-22 |
| I.4-16 Geological Section for Seismic Line SL: CD-9 | I-F-22 |
| I.4-17 Geological Section for Seismic Line SL: CD-10 | I-F-23 |
| I.4-18 Geological Section for Seismic Line SL: TD-1 | I-F-24 |
| I.4-19 Geological Section for Seismic Line SL: DD-2 | I-F-24 |
| I.4-20 Geological Section for Seismic Line SL: CP-2-P | I-F-25 |
| I.4-21 Geological Section for Seismic Line SL: CP-2-C | I-F-26 |
| I.4-22 Geological Section for Seismic Line SL: CP-3-P | I-F-27 |
| I.4-23 Geological Section for Seismic Line SL: CP-3-C | I-F-27 |
| I.4-24 Geological Section for Seismic Line SL: TP-2-P | I-F-28 |
| I.4-25 Geological Section for Seismic Line SL: TP-2-C | I-F-29 |
| I.4-26 Geological Section for Seismic Line SL: TP-3-C | I-F-30 |
| I.4-27 Geological Section for Seismic Line SL: TP-4-C | I-F-31 |
| I.4-28 Geological Section for Seismic Line SL: TP-5-C | I-F-32 |
| I.4-29 Geological Section for Seismic Line SL: TP-1-P | I-F-33 |
| I.4-30 Geological Section for Seismic Line SL: TP-1-C | I-F-33 |
| I.5-1 Lugeon Map for SL: CD-1 | I-F-34 |
| I.5-2 Lugeon Map for SL: CD-2 | I-F-35 |
| I.5-3 Lugeon Map for SL: CD-3 | I-F-35 |
| I.5-4 Lugeon Map for SL: CD-4 | I-F-36 |
| I.5-5 Lugeon Map for SL: CD-5 | I-F-36 |
| I.5-6 Lugeon Map for SL: CD-6 | I-F-37 |
| I.5-7 Lugeon Map for SL: CD-8 | I-F-38 |
| I.5-8 Lugeon Map for SL: CD-9 | I-F-38 |

| | <u>Page</u> |
|------------------------------------------------------------------------------------------------|-------------|
| I.5-9 Lugeon Map for SL: TD-1 | I-F-39 |
| I.5-10 Lugeon Map for SL: TD-2 | I-F-39 |
| I.5-11 Lugeon Map for SL: CP-2-P | I-F-40 |
| I.5-12 Lugeon Map for SL: TP-2-P | I-F-41 |
| I.6-1 Unconfined Compressive Strength versus Unit Weight | I-F-42 |
| I.6-2 Unconfined Compressive Strength versus Effective Porosity | I-F-45 |
| I.6-3 Unconfined Compressive Strength versus Tangent Modulus of Static Elasticity | I-F-48 |
| I.6-4 Triaxial Compression Test Data | I-F-51 |
| I.7-1 Geological Profile for Talawakelle Headrace Tunnel | I-F-55 |

APPENDIX I

GEOLOGY

I.1 Topography and General Geology

I.1.1 General

The Study area is situated in central Sri Lanka. Topographically, the area belongs to the deeply dissected highest peneplane. As a result, overall undulation is marked.

For the subject Study, a relative relief map was prepared by imposing a 2km grid on a restored map drawn from 1:20,000 scale topomapping of the area and determining relative relief from the restored contour lines (refer to FIG.I.1-1)

Maximum relative relief was 850m/4km² and minimum relative relief was 150m/4km². A mountainous sector of large relative relief in excess of 400m/km² occupies much of the northern half of the Study area.

A parallel drainage pattern is dominant in the northern half of the Study area, while a rectangular drainage pattern is prevalent in the southern portion. (see FIG. I.1-2)

In terms of geology, relative relief is large in the area of charnockite distribution. This is particularly true of the periphery of the charnockite area, where relative relief is in excess of 600m/4km². Topographically, this indicates that charnockite comprises caprock.

Furthermore, charnockite comprises a syncline in the Pundal oya catchment, creating a parallel drainage pattern in the catchment.

I.1.2 Topography

Mountains

Mountainous area of high relief is distributed in the northern half and the southern extremity of the area covered by 1:20,000 topomapping. Mountainous area of intermediate and small relief is found along the Kotmale river (see FIG. I.1-3).

The high relief mountainous sector at the southern edge of the Study area comprises mesas and buttes. The fact that charnockite does not

weather easily indicates that topographically it constitutes caprock. This fact in turn indicates that as a result of topographical processes such as rock fall, etc., numerous blocks have been formed at the edge of the area distributed with charnockite.

The most prevalent direction of river flow in the Study area is NW. Next in predominance are NE and NNE. In certain limited locales, EW, NS flows are common.

Slopes

Almost all slopes at mountain summits are comprised of charnockite forming mesas and buttes. Slopes on the flanks of mountains, as with the case on the left bank of the Pundal oya, constitute landslide topography in many instances.

Slopes at the foot of mountains consist almost entirely of creeping and/or sliding of rock debris, and comprise colluvial slopes continuing smoothly from mountainside slopes.

Rivers; valley bottoms

Mountainous area of intermediate~low relief is distributed along the Kotmale river. Geologically, this is due to occurrence of easily decomposed khondalite group.

This sector is characterized by only minor development of river terrace, despite overall mature topography. This is considered as resulting from the fact that fluctuation in standard surface for erosion is limited due to the subject area being located far from the sea and the absence of fault activity accompanying vertical displacement.

I.1.3 General Geology

Within the Study area, upper charnockite group occurs at ridgelines of mountain chains surrounded by steep slope topography, while khondalite group is distributed at the foot of mountains forming gentle slopes.

Underlying the khondalite group, thick formation of charnockite is found along the valley of the Kotmale river. Waterfalls such as St. Clair and Devon falls occur at the boundary of these two formations.

Stratigraphic succession of the Study area may be described as follows:

| | | |
|-------------------|----------|------------------------------|
| Upper charnokite: | 300m+ | forms steep slope and cliffs |
| Khondalite: | 250~600m | forms gentle slopes |
| Lower charnokite: | 300m+ | forms steep slopes; gorges |

Stratigraphically, traceable key bed consists of quartzite bed contained within the upper part of khondalite group formation.

Details of this stratification are given in FIG.3.2-2 of the main report.

I.2 Investigations

I.2.1 General

In the course of the subject Study, aerophotography of the entire Study area, general surface geologic survey, detailed geologic investigation of the structure sites, test boring (along with Lugeon testing), as well as laboratory testing utilizing drill core samples were carried out. The results of these various studies and tests are discussed in detail in chapters 3 and 4 of this appendix. In this section, the results of Lugeon testing and laboratory testing will be examined.

Also, site location, drilling depth, survey line length, etc. for seismic prospecting will be indicated by means of figures and tables.

I.2.2 Core Drilling

Thirty-seven boreholes were drilled for a total of 1,778.98m. Details of this test drilling are presented in the following tables. Drill sites are indicated in FIG.I.2-1 to - 5 along with seismic survey lines. Drilling logs for all cores are presented in the Data Book.

TABLE I.2-1
(1/3)

DRILLING DATA

| Location | Drilling Hole No. | Coordinates North East | Ground Height(m) | Drilled Depth (m) | Water 1/ Pressure Test(m) |
|--------------------|-------------------|------------------------------|------------------|-------------------|------------------------------|
| Caledonia Dam Site | CD - 1 | 189,140.49 192,705.11 | 1,301.592 | 20.59 | 20 |
| | CD - 2 | 189,337.00 192,830.59 | 1,377.271 | 30.08 | 30 |
| | CD - 3 | 189,318.93 192,783.98 | 1,366.901 | 40.09 | 40 |
| | CD - 4 | 189,284.19 192,713.54 | 1,347.146 | 40.11 | 40 |
| | CD - 5 | 189,238.44 192,606.67 | 1,310.582 | 50.28 | 50 |
| | CD - 6 | 189,245.74 192,560.49 | 1,335.274 | 40.00 | 40 |
| | CD - 7 | 189,210.47 192,526.75 | 1,371.780 | 40.05 | 40 |
| | CD - 8 | 189,233.00 192,476.61 | 1,385.291 | 40.39 | 40 |
| | CD - 9 | 189,360.80 192,653.76 | 1,325.843 | 29.50 | 20 |
| | CD - 10 | 189,309.33 192,583.25 | 1,300.202 | 40.10 | 40 |
| | CD - 11 | 189,485.33 192,591.31 | 1,353.816 | 50.47 | 50 |
| | CD - 12 | 189,359.26 192,527.94 | 1,331.115 | 40.17 | 40 |
| | CD - 4 - A | 189,261.32 192,695.75 | 1,328.496 | 50.55 | 50 |
| | Sub-total | | | 512.38 | (500) |
| Caledonia Intake | CI - 1 | 189,180.85 192,854.03 | 1,337.317 | 24.85 | - |
| | Sub-total | | | 24.85 | - |

1/ A water pressure test was carried out every 5m in depth.

TABLE I.2-1
(2/3)

DRILLING DATA

| Location | Drilling Hole No. | Coordinates North East | Ground Height(m) | Drilled Depth(m) | Water ^{1/} Pressure Test(m) |
|-------------------------|-------------------|--------------------------|------------------|------------------|--------------------------------------|
| Caledonia Saddle | CS - 1 | 188,875.68 192,542.13 | 1,369.136 | 32.35 | 30 |
| | CS - 2 | 188,829.74 192,511.49 | 1,349.065 | 30.45 | 30 |
| | CS - 3 | 188,742.78 192,496.88 | 1,366.855 | 30.00 | 30 |
| | CS - 4 | 188,961.09 192,487.22 | 1,364.810 | 30.55 | 30 |
| | CS - 5 | 188,845.01 192,448.33 | 1,338.195 | 20.20 | - |
| | CS - 6 | 188,934.95 192,145.61 | 1,271.778 | 17.15 | - |
| | Sub-total | | | 160.70 | 120 |
| Caledonia Quarry | CQ - 1 | 189,321.70 193,246.09 | 1,425.899 | 40.14 | |
| | CQ - 2 | 188,430.86 193,424.44 | 1,355.958 | 40.08 | |
| | Sub-total | | | 80.22 | |
| Caledonia Power Station | CP - 1 | 190,754.96 190,614.24 | 1,299.214 | 150.50 | 100 (Under 50m) |
| | CP - 2 | CANCELLED | | | |
| | Sub-total | | | 150.50 | |
| Caledonia Surge Chamber | CC - 1 | 190,717.03 190,746.34 | 1,340.131 | 70.40 | |
| | CC - 2 | CANCELLED | | | |
| | Sub-total | | | 70.40 | |
| Caledonia Total | | | | 999.05 | 720 |

^{1/} A water pressure test was carried out every 5m in depth.

TABLE I.2-1
(3/3)

DILLING DATA

| Location | Drilling Hole No. | Coordinates North East | Ground Height(m) | Drilled Depth(m) | Water ^{1/} Pressure Test(m) |
|---------------------------|-------------------|------------------------------|------------------|------------------|--------------------------------------|
| Talawakelle Dam | TD - 1 | 190,063.49 187,937.73 | 1,239.079 | 30.81 | 30 |
| | TD - 2 | 193,076.72 187,847.49 | 1,199.448 | 19.63 | 20 |
| | TD - 3 | 193,063.49 187,937.73 | 1,195.380 | 19.99 | 20 |
| | TD - 4 | 193,076.72 187,847.49 | 1,206.143 | 28.96 | 20 |
| | TD - 5 | 192,748.73 187,893.87 | 1,200.600 | 30.58 | 20 |
| | TD - 6 | 192,623.64 187,867.66 | 1,197.542 | 25.90 | 20 |
| | Sub-total | | | 155.87 | 130 |
| Talawakelle Power Station | TP - 1 | CANCELLED | | | |
| | TP - 2 | 204,320.21 187,505.46 | 941.695 | 351.57 | 50 (Under 300m) |
| | TP - 2' | 204,467.32 187,303.85 | 800.722 | 50.87 | |
| | Sub-total | | | 402.44 | 50 |
| Talawakelle Surge Chamber | TC - 1 | CANCELLED | | | |
| | TC - 2,2' | 203,996.94 187,991.91 | 1,243.015 | 100.51 | |
| | Sub-total | | | 100.51 | |
| Talawakelle Penstock | TS - 1 | 204,149.03 187,733.94 | 1,024.046 | 121.11 | |
| | Sub-total | | | 121.11 | |
| Talawakelle Total | | | | 779.92 | 180 |
| GRAND TOTAL | | | | 1,778.98 | 900 |

^{1/} A water pressure test was carried out every 5m in depth.

I.2.3 Seismic Prospecting Survey

In the subject survey, seismic prospecting was performed along 23 survey lines for a total of 12,485m (see following table). Survey line and drill site locations are indicated in FIG.1.2-1.to-5.

TABLE I.2-2 SEISMIC PROSPECTING DATA

| Location | No. | Length (m) | Description | Direction |
|--------------------------------|--------|------------|--------------------------------|-----------|
| Caledonia Dam Site | CD-1 | 550 | Upper Alternative Axis | N65°00'E |
| | CD-2 | 400 | Lower Alternative Axis | N35°00'E |
| | CD-3 | 300 | Right Bank (Parallel to River) | N24°30'W |
| | CD-4 | 300 | Left Bank (Parallel to River) | N26°00'W |
| | CD-5 | 350 | Left Bank Ridge to Saddle | N33°00'W |
| | CD-6 | 460 | Spillway Profile | N75°00'W |
| | CD-7 | 115 | Spillway Cross | N15°00'E |
| | CD-8 | 300 | Saddle Dam Axis | N18°30'E |
| | CD-9 | 395 | Landslide Area on Right Bank | N25°00'E |
| | CD-10 | 3,630 | CD-5 Cross | N62°00'E |
| Caledonia Power Station Site | CP-2-P | 1000 | Route No.2 Profile | N66°00'W |
| | CP-2-C | 805 | Route No.2 Cross | N24°00'E |
| | CP-3-P | 1030 | Route No.3 Profile | N43°00'E |
| | CP-3-C | 2,985 | Route No.3 Cross | N46°00'W |
| Talawakelle Dam Site | TD-1 | 200 | Lower Alternative Axis | N89°00'W |
| | TD-2 | 400 | Upper Alternative Axis | N12°00'E |
| Talawakelle Power Station Site | TP-1-P | 2000 | Route No.1 Profile | N11°00'W |
| | TP-1-C | 300 | Route No.1 Cross | N79°00'E |
| | TP-2-P | 800 | Route No.2 Profile | N55°30'W |
| | TP-2-C | 1380 | Route No.2 Cross | N35°00'E |
| | TP-3-C | 300 | Route No.2 Cross | N35°00'E |
| | TP-4-C | 345 | Route No.2 Cross | N35°00'E |
| | TP-5-C | 5,470 | Route No.2 Cross | N35°00'E |
| Total | | 12,485 | | |

I.2.4 Laboratory Testing

Laboratory tests for drilled cores were carried out as follows.

TABLE I.2-3 LABORATORY ROCK TEST

| Test item | Test quantity | | | | Total |
|--------------------------|--------------------|-----------------------|----------------------|----------------------|-------|
| | Caledonia dam site | Caledonia saddle site | Talawakelle dam site | Talawakelle P/S site | |
| Mechanical test | | | | | |
| Uniaxial | 28 | 15 | 10 | 16 | 699 |
| Triaxial | 5 | 1 | 1 | 2 | 9 |
| Tensile | 7 | 2 | 2 | 3 | 14 |
| Sonic | 6 | 2 | 2 | 2 | 12 |
| Physical properties test | | | | | |
| Bulk density | 50 | 26 | 15 | 25 | 116 |
| Porosity | 50 | 26 | 15 | 25 | 116 |
| Specific gravity | 50 | 26 | 15 | 25 | 116 |

I.3 Geomorphological Study

I.3.1 Introduction

On the basis of 1:20,000 topo-map prepared during the Study, a restored map and drainage pattern map of the Study area were drawn up. Aerial photographs were also studied using stereoscope.

As a result of these efforts, lineaments in the Study area and distribution of steep mountainous terrain, assumed to consist of massive compact formation, were identified; and a tentative survey program was drawn up prior to the field work.

A summary of geomorphological study is presented below.

Drainage pattern

Drainage patterns in the Study area are classified as follows:

- a. Parallel
- b. Coarse rectangular
- c. Fine rectangular
- d. Dendritic

Parallel drainage pattern is considered as generally occurring where dip of strata and sloping of topography coincide. Rectangular drainage often occurs in holocrystalline rock where regular joint/fissure system is well developed. Dendritic drainage on the other hand exhibits differing geologic conditions than the previously described two types of pattern, although said conditions appear to be of no one specific classification of lithofacies or geostructure.

Lineament

Lineaments as observed on the aerial photographs are predominantly oriented first in a general NE-SW direction and secondly in a NW-SE direction. Analyses of the restored map and the drainage pattern indicated the two general attitudes of lineaments. These are the NE-SW trending lineaments coinciding with several lineaments identified on the aerial photographs and the NW-SE trending lineaments which cross some of the NE-SW lineaments. These two groups of lineament may represent conjugate faults created at the same geologic age by N-W or E-W compressional stress.

Some lineaments which are rather short and discontinuous and trending generally to the N-S and E-W directions were observed both on aerial photographs and on the restored map. The short and discontinuous N-S / E-W lineaments may represent the tension joints and the stress release joints resulting from either N-S or E-W major stress directions.

River flows in almost every case are governed by the lineaments of the Study area which in some cases form straight valleys of several kilometer length. Lineament No. 2 creates crank-curved creeks in the southeast portion of the figure.

This type of topography is commonly seen where active faults occur, and may suggest recent lateral movement along lineament No. 2. Accordingly, it was concluded that this possibility warranted detailed investigation.

I.3.2 Ground Truth and Conclusions

Results of the field survey are as follows.

Drainage patterns

The parallel drainage pattern characteristically appears where charnockite group moderately dips in the same direction as topographical sloping. Particularly in the vicinity of the Pundal oya syncline, an extremely marked parallel pattern was identified.

The fine rectangular drainage pattern occurs in areas of complex erosion on the charnockite area. No relationship between geo-structure and topographical sloping is evident.

Occurrence of the coarse rectangular drainage pattern shows close correlation to distribution of khondalite group.

The dendritic drainage pattern is seen in areas where khondalite and charnockite group occur together. In such areas, dip of the strata is low to moderate.

It was discovered that the above described drainage patterns closely reflect the geology of the area. The boundaries of drainage patterns generally correspond closely to the lineaments in the figure.

Lineaments

On the surface, only a limited number of sheared zones were identified, and no obvious fault displacement along the lineaments was observed. The NW-SE lineament referred to as lineament No. 2 was found to represent folding axes.

The crank-curved creeks considered to suggest active faulting with lateral movement were carefully studied in the field. However, no evidence of active fault was found except for small landslides along lineament No. 2. Micro-earthquake study conducted by CECB during February 1982 in the Kotmale dam area suggests that the studied area is stable and quiet in terms of seismology.

Judging from the above mentioned field observation, the complicated morphostructure of the area may have been caused by a combined process of folding, deep penetrating weathering along the lineament, and succeeding erosion and faulting.

Since some of the probable faults revealed by the morphostructural study will be crossing the sites for some of the proposed Project structures, further field investigations will be allocated in critical areas to confirm the existence and nature of the geological structures so that appropriate measures may be adopted before design is finalized.

I.4 GEOLOGY AT MAJOR STRUCTURE SITES

I.4.1 General

In the course of the subject Study, a total of 1778.98m of mechanical boring and 11,585m of seismic prospecting were conducted centering on candidate sites for the major structures in order to identify geologic conditions.

Sites for boring and seismic prospecting are indicated in figures I.2-2 to 5. Location coordinates, elevation, borehole depth, etc. for test boring, and survey line length, orientation, etc. for seismic prospecting are shown in tables I.2-1~I.2-2. Geological route map and geological structure map both for overall Project area are shown in FIG.I.4-1 and FIG.I.4-2, respectively.

On the basis of the results of this testing as well as surface geologic reconnaissance (see the route map), conditions and problems relevant to the geology at the sites for major structures will be discussed in this chapter.

On the basis of seismic prospecting, the velocity structure of the surveyed area is broadly classified into 5 layers. A comparison of these velocity layers and the results of core boring reveal a general correspondence between geology and rock class (weathering classification) as shown in the following Table.

TABLE I.4-1 VELOCITY LAYER STRUCTURE AND GEOLOGICAL CLASSIFICATION

| Velocity Layer | Velocity (km/sec) | Geology | Rock Classification |
|-------------------|-------------------|---------------------------------------|---------------------|
| 1st Layer | 0.25~0.35 | Topsoil, weathered soil | D |
| 2nd Layer | 0.5~0.8 | Highly weathered rock, talus deposits | D |
| 3rd Layer | 1.0~1.5 | Highly weathered rock | CL |
| 4th Layer | 2.0~2.4 | Weathered rock | CM |
| 5th Layer | 5.0~6.2 | Fresh rock | B~A |
| Low Velocity Zone | 2.5~4.0 | Sheared zone | CL~CH |

TABLE I.4-2 VELOCITY LAYER AT CALEDONIA DAM SITE

| Line Velocity Layer | CD-1 | CD-2 | CD-3 | CD-4 | CD-5 | CD-6 | CD-7 | CD-8 | CD-9 | CD-10 |
|---------------------------|--------------------|----------------------|-------------------|------------------|----------------------|--------------------------------|---------------------|----------------------|-------------------|-------------------|
| 1st Layer | 0.25~0.35 (0~6) | 0.25~0.3 (1~3) | 0.3~0.35 (0~4) | 0.3 (0~2) | 0.3 (1~4) | 0.3~0.35 (1~5) | 0.3 (0~3) | 0.3~0.35 (0~5) | 0.3 (0~3) | 0.3 (1~3) |
| 2nd Layer | 0.5~0.7 (0~11) | 0.5~0.7 (2~10) | 0.5~0.7 (1~9) | 0.5~0.7 (1~5) | 0.5~0.7 (4~10) | 0.5~0.7 (1~7) | 0.5~0.7 (0~3) | 0.5~0.7 (5~12) | 0.5~0.7 (2~8) | 0.5~0.8 (2~11) |
| 3rd Layer | 1.2~1.4 (0~9) | 1.0~1.2 (1~12) | 1.2~1.4 (0~9) | non- existent | 1.0~1.2 (4~17) | 1.0~1.5 (4~10) | 1.2~1.4 (0~5) | 1.0~1.4 (2~13) | 1.0~1.2 (0~8) | 1.0~1.2 (0~10) |
| 4th Layer | 2.0~2.2 (2~11) | 2.2~2.4 (2~10) | 2.0~2.4 (7~12) | 2.2~2.4 (2~6) | 2.2~2.4 (7~18) | 2.2~2.4 (3~10) | 2.2~2.4 (4~5) | 2.2~2.4 (5~16) | 2.0~2.2 (8~13) | 2.2~2.4 (4~15) |
| 5th Layer | 5.3, 6.0~6.2 | 5.1~5.3 5.6~6.0 | 6.0 | 6.0 | 5.8~6.0 | 5.2~5.6 | 5.0~6.0 | 5.3~5.8 | 5.7~6.0 | 5.4, 6.0~6.2 |
| Low velocity zone | 2.6 (7) | 2.5, 2.8 (8) (20) | 3.3 (20) | | 1.2, 2.8 (5) (20) | 2.8, 2.8, 3.0 (5) (10) (10) | 2.5, 2.5 (5) (5) | 2.5, 2.8 (5) (15) | 3.2 (5) | 2.4 (1.5) |

Note: velocity is in km/sec
 values in () represent layer thickness in m
 values in () of low velocity zone are width in m

TABLE 1.4-3 VELOCITY LAYER AT TALAWAKELLE DIVERSION DAM SITE

| Line | TD-1 | TD-2 |
|-------------------|-----------------------|-----------------------|
| Velocity Layer | | |
| 1st Layer | 0.3 (0 ~ 6) | 0.3 (1 ~ 4) |
| 2nd Layer | 0.5 ~ 0.7 (0 ~ 10) | 0.5 ~ 0.7 (1 ~ 8) |
| 3rd Layer | 1.2 ~ 1.4 (8 ~ 14) | 1.2 ~ 1.4 (2 ~ 6) |
| 4th Layer | 2.0 ~ 2.2 (4 ~ 6) | 2.0 ~ 2.2 (3 ~ 10) |
| 5th Layer | 5.0 | 5.0 |
| Low velocity zone | | |

Note: Velocities are in km/sec
 Values in () are thickness in m

TABLE I.4-4 VELOCITY LAYER AT CALEDONIA P/S SITE

| Line | CP-2-P | CP-2-C | CP-3-P | CP-3-C |
|-------------------|-----------------------|-------------------|---------------------------------|-------------------|
| Velocity Layer | | | | |
| 1st Layer | 0.3~0.35 (0~8) | 0.3~0.35 (0~6) | 0.3 (0~7) | 0.3 (0~2) |
| 2nd Layer | 0.5~0.7 (0~10) | 0.5~0.7 (0~10) | 0.5~0.7 (0~9) | 0.5~0.7 (0~6) |
| 3rd Layer | 1.0~1.2, 1.5 (0~6) | 1.2~1.4 (0~8) | 1.2~1.4 (0~15) | 1.2~1.4 (0~12) |
| 4th Layer | 2.2~2.4 (3~10) | 2.2~2.4 (3~14) | 2.2~2.4 (2~11) | 2.2~2.4 (5~10) |
| 5th Layer | 4.8, 5.7~6.0 | 4.9, 5.8~6.2 | 5.4~5.9 | 5.4~5.6 |
| Low velocity zone | | 2.8 (10) | 3.0, 3.4, 3.4 (20) (10) (20) | 2.8 (1~5) |

Note: Velocity is in km/sed
 Values in () are layer thickness in m
 Values in () of low velocity zone are width in m

TABLE I.4-5 VELOCITY LAYER AT TALAWAKELLE P/S SITE

| Line Velocity Layer | TP-1-P | TP-1-C | TP-2-P | TP-2-C | TP-3-C | TP-4-C | TP-5-C |
|---------------------------|--------------------|---------------------------|----------------------------|--------------------|------------------|--------------------|-------------------|
| 1st Layer | 0.3 (0~3) | 0.3 (1~2) | 0.3 (0~4) | 0.3 (0~4) | 0.3 (0~5) | 0.3 (0~3) | 0.3 (0~3) |
| 2nd Layer | 0.5~0.7 (0~10) | | 0.5~0.7 (0~8) | 0.5~0.7 (0~8) | 0.5~0.7 (1~7) | 0.5~0.7 (0~6) | 0.5~0.7 (0~10) |
| 3rd Layer | 1.2~1.4 (0~13) | 1.2~1.4 (5~10) | 1.0~1.2 (0~4) | 1.2~1.4 (0~10) | 1.2~1.4 (0~4) | 1.0~1.2 (3~20) | |
| 4th Layer | 2.2~2.4 (2~13) | 2.2~2.4 (4~11) | 2.0~2.2 (2~12) | 2.2~2.4 (4~20) | 2.0~2.2 (4~8) | 2.2~2.4 (8~16) | 2.2~2.4 (4~12) |
| 5th Layer | 4.5~4.7 5.6~6.0 | 5.0~5.8 | 5.0~5.9 | 5.3~6.2 | 5.2 | 4.0, 5.0~5.6 | 5.0~5.4 |
| Low velocity zone | 2.4~3.2 (10~20) | 2.6,2.5,2.7 (5)(5)(10) | 3.5,2.5,2.9 (30)(5)(10) | 2.9~3.9 (10~40) | | 2.2,2.4 (5)(10) | 2.7 (15) |

Note: velocity is in km/sec
 values in () represent layer thickness in m
 values in () of low velocity zone are width in m

I.4.2 Caledonia Dam Site

I.4.2.1 Surface Reconaissance (See attached route map FIG.I.4-3)

Geological map for the Caledonia dam area is presented in FIG.I.4-3. Velocity layer structures at the each structure site are presented in Tables I.4-2 to I.4-5. Outcropping of good base rock is seen on the left bank of the upstream-alternative site, on the downstream side of the downstream-alternative site and on the downstream right bank at the confluence of the Agra and Dambagastalawa rivers. On the other hand, landslide topography is in evidence on the right bank side downstream (about 75m) of the upstream-alternative site, and moderately thick talus deposits were found on both banks of upstream (about 250m) of the upstream-alternative site

Age of landsliding is considered to be old and type is bottleneck. At the central portion and the toe of the landslide zone, relatively thick piling of rock debris is anticipated.

The principal component of the geostructure of the dam site area is the NW-SE trending anticlinal axis which passes the riverbed portion of the upstream and downstream-alternative sites. This anticlinal axis is diagonally intersected by a N-S / NNW-SSE trending fold axis. In addition, a N60°E trending fault (15m throw) is confirmed in the vicinity of the downstream-alternative site. A N35°E trending fault is estimated to exist about 200m upstream of the upstream-alternative site, where riverbed outcrops disappear suddenly.

I.4.2.2 Results of Drilling and Seismic Prospecting

At the upstream-alternative site shown in LINE SL:CD-1, a thin bed (1~3m) of highly weathered rock (D~CL class) is located on the left bank slope. Base rock (CM class or better) is distributed at shallow depth. In contrast, a 5~15m thick bed of highly weathered rock occurs on the right bank side. The surface portion of this bed consists of 1~6m thick deposit of debris. Base rock is located well below the surface at GL - 10~20m.

It is estimated on the basis of seismic prospecting that a 7m wide, low velocity (2.6km/s) zone is present in the vicinity of the survey point 520m. Results of boring no. CD-3 also indicate a thick bed (25~30m wide)

of highly weathered rock in the same vicinity. These conditions suggest the presence of a sheared zone. This low velocity zone is assumed from results of seismic prospecting (see figures 2,9) to have N45°W trending, and to run roughly parallel to the anticlinal axis passing the riverbed portion at the site.

Boring results reveal that lithofacies at the upstream-alternative site consists principally of intermediate charnockite, often intercalated with biotite gneiss, felsic gneiss, granitic gneiss, etc. As shown in LINE SL:CD-1, these rock types comprise a continuous formation.

A thin bed (0~3m thick) of highly weathered rock is located on both bank slopes at the downstream-alternative site (refer to LINE SL:CD-2). On the right bank, rock outcrop 30m high forms a steep cliff. At the upper portion of slopes on both banks, 1330m~1360m on the left bank and over 1350m on the right bank, the thickness of weathered rock becomes 10~20m.

Results of seismic prospecting reveal a low velocity layer (2.5~2.8km/s) in the vicinity of the survey point 350m. This is considered to be an extension of the sheared zone seen at the upstream-alternative site. A N60°E trending small drag fault is confirmed at the downstream edge of the above described steep cliff.

The formation shown by solid line in the figure corresponds to the same strata as mentioned for the upstream-alternative site, and is exposed at the central and lower portions of the steep cliff. This formation exhibits clear 30cm thick banding and is more readily susceptible to weathering and erosion in comparison to intermediate charnockite.

LINE SL:CD-3 (right bank) and LINE SL:CD-4 (left bank) are cross-sections roughly parallel to the Kotmale oya. Both have a starting point at the downstream side (0m on the seismic survey line). The solid line in the figures indicate the above described banded formation. Overall formation is somewhat undulated. According to LINE SL:CD-1, the interval 0m~170m on the survey line corresponds to landslide zone, and is anticipated to consist of debris with maximum bed thickness of 12m (in vicinity of survey point 45m).

At interval 0m~120m of the survey line, the base rock is found at GL-1~12m, directly below the bed of debris. In contrast, a bed of highly weathered rock, 3~13m thick, is seen below the debris and surface soil at

interval 120~300m. Depth of base rock at this interval tends to be deep at GL-5~20m. A low velocity zone (3.3km/s) is confirmed at interval 50m~70; however, degree of continuity is unclear.

In LINE SL:CD-4, bed of surface soil and heavily weathered rock (D~CL class) is 1~6m thick, and base rock is overall located at shallow depth.

LINE SL:CD-9 presents a profile of the landslide zone. According to the figure, the slide plane roughly parallels topography, and thickness of debris is 3~10m. A 2~5m thick bed of CL class rock (1.0~1.2km/s) is located below the debris (at survey stations 15~55m of the survey line, base rock is directly located beneath the debris), and base rock is generally located at GL-7~15m. However, at borehole no. 9, a 25m thick bed of highly weathered rock is confirmed. Thus, base rock depth shows considerable variation depending on the location.

I.4.3 Caledonia Dam Site Saddle

I.4.3.1 Surface Reconnaissance (See route map FIG.I.4-3)

Although one portion of relatively good CM class or better rocks outcropped at one part of the streambed and slope of the ravine which flows NW-SE, from the saddle, almost all of the site area including along national highway A-7 is outcropped with argillized D~CL class rock. Also, talus deposits are seen distributed on parts of slopes on both sides of the ravine.

The structure of the area is governed by the afore-described anticlinal axis which passes the riverbed of the Kotmale oya and the synclinal axis extending NW-SE in the vicinity about 300m south of the saddle. Strike and dip of bedding are N40~70°W and 10~45°S, respectively.

A fault is confirmed at one location on the right bank of the ravine slope, and exhibits strike of N50°W and dip of 60°S.

I.4.3.2 Results of Drilling and Seismic Prospecting

LINE SL:CD-8 presents a cross section of the saddle area. According to the figure, thickness of highly weathered rock (class D~CL:

0.5~1.4km/s) at the site is roughly 12~30m. Base rock is found at considerable depth.

At survey points 130~135m and 240~255m, low velocity zones (2.5~2.8km/s) are found. The former is considered to correspond to the fault identified during the reconnaissance. Other survey lines also confirmed the presence of these low velocity zones. The latter zone is estimated to extend N60°W.

Lithofacies at the saddle consist of irregular alternation of felsic gneiss, basic charnockite, intermediate charnockite and granitic gneiss. The solid line in the figure represents felsic gneiss.

Results of boring indicate the crack-zones with slickenside and striation at all of the CS-1 ~ CS-3 boreholes, suggesting the occurrence of structural movement such as faulting, etc.

LINE SL:CD-6 is a cross section of the afore-described ravine. According to the figure, the bed of highly weathered rock is thin (2~3m) at the riverbed and thick at slopes and ridges (10~20m).

Results of seismic prospecting indicate low velocity zones (2.8~3.0km/s) at survey points 120~125m, 150~160m, and 400~410m.

The zones between survey points 150~400m correspond to the low velocity zones indicated in LINE SL:CD-8.

At boreholes CS-5 and CS-6, crack-zones identical to those at the saddle are identified.

Lithofacies identified by boring exhibit interbedding as seen at the saddle. The solid line and dotted line in the figure represent basic charnockite (biotite gneiss) at survey points 0~170m, granitic gneiss identified during site reconnaissance at 195~330m, and felsic gneiss ~ garnet gneiss indicated in FIG.I.4-9 at 410~450m.

LINE SL:CD-7 shows a section which crosses that in LINE SL:CD-6. The low velocity zone seen here corresponds to the one described in the previous section. The solid and broken lines in the figure indicate the granitic gneiss confirmed during reconnaissance.

LINE SL:CD-5 shows the LINE cross-section. In the figure, the thickness of the bed of heavily weathered rock is 8~10m at survey points

0~40m and 215~235m. At other intervals, the said bed is extremely thick at 25~30m, with base rock located at considerable depth.

The results of seismic prospecting indicate low velocity zone (2.8km/s) at survey points 285~305m. However, actual orientation of this zone (tentatively shown in the figure at N50°W, 60°S) could not be confirmed.

The solid line and dotted lines at survey points 185~275m represent the boundary between the afore-discussed interbedded formation and the underlying intermediate charnockite. At survey points 205~350m, the solid line indicates the felsic gneiss shown in LINE SL:CD-8.

LINE SL:CD-10 presents a cross section from the Kotmale oya in the direction of figures 6 and 7. According to the figure, the thickness of the bed of highly weathered rock fluctuates greatly, being 10~15m on the slope at survey points 0~170m, reaching a maximum of 25m at the ridge at 170~270m, and thinning to 2~4m at 270~450m (near the streambed of the ravine).

A low velocity zone is seen at survey points 85~100m, corresponding to the northern side low velocity zone shown LINE SL:CD-8. The solid and dotted lines in LINE SL:CD-10 indicate granitic gneiss identified during reconnaissance at survey points 0~115m, the boundary between upper and lower formations shown in LINE SL:CD-5 at 135~365m, and the banded formation (biotite gneiss and felsic gneiss) indicated in LINE SL:CD-1 at 275~450m respectively.

I.4.4 Talawakelle Dam Area

4.4.1 Surface Reconnaissance (See attached route map FIG.I.4-5)

The riverbed and right bank at the downstream side including the downstream-alternative site exhibit outcropping of relatively good (CM class or better) rock. In contrast, recent river deposits (alluvial bed) are seen at the riverbed at the upstream-alternative site, with deeply weathered rock of D~CL class identified on both banks.

Also, small landslide zones are seen about 150m and 250m upstream of the upstream-alternative site on the right bank.

The major component of the geostructure is the NW-SE trending St. Clair syncline running about 800m northeast of Talawakelle town. Nevertheless, the minor folding structure with N-S axis (Talawakelle structural bend) located at the dam site and vicinity is dominant, and largely governs the strike and dip of the rock formation in the immediate area.

I.4.4.2 Results of Drilling and Seismic Prospecting

Results of boring at the downstream-alternative site LINE SL:TD-1 show that the thickness of the bed of highly weathered rock (D~CL class) is somewhat great at 10m on the left bank and 10~20m on the right bank; while tending to be thinner in the direction of the upper slope on the right bank. Seismic prospecting indicates results generally corresponding to those of test boring, with a highly weathered zone (0.5~1.4km/s) of 10~15m thickness identified which becomes thinner in the direction of the right bank upper slope.

No low velocity zone of note was confirmed in this cross-section.

Lithofacies identified by test boring consist of principally intermediate charnockite, partially intercalated with felsic gneiss and basic charnockite. Based on the small fold structure identified during field reconnaissance, the solid line in the figure represents formation assumed to be an extension of the felsic gneiss confirmed at TD-4 boring.

Results of boring and seismic prospecting at the upstream-alternative site (see LINE SLITD-2) indicate that the thickness of the bed of highly weathered rock (D~CL class; 0.5~1.4km/s) is extremely great at 25m on both banks. The highly weathered zone extends to 13m depth in the river bed.

Seismic prospecting shows the presence of a low velocity zone (velocity unclear) which possibly extends in the same direction as the Kotmale oya channel (roughly E-W direction).

Lithofacies of the site area is considered to consist of irregular interbedding of intermediate charnockite and felsic gneiss, basic charnockite, etc. (intermediate charnockite is dominant). The solid line in the figure indicates felsic gneiss and basic charnockite confirmed at TD-6, and is expressed reflecting dip and strike observed at the surface.

I.4.5 Caledonia Power Station Site

I.4.5.1 Reconnaissance (see attached route map FIG.I.4-6)

Both an upstream-alternative site and a downstream-alternative site are considered for the Caledonia power station. At the vicinity of the upstream-alternative site, continuous outcropping of good base rock is seen on the left bank slope of the Kotmale oya. On the right bank, however, little outcropping of good rock is present. However, due to the fact that slightly weathered CL class rock is seen at side cuts along the road route, underlain in parts by CM class or better rock, the depth of base rock on the right bank is estimated to be relatively shallow. This assumption is further backed up by the results of seismic prospecting as discussed below.

The principal components of the geostructure of the upstream-alternative site the St. Clair syncline extending NW-SE about 150m above the site and the syncline (same syncline as that to the south of the Caledonia saddle) trending NW-SE 900m to the south of the site. An anticline is estimated to exist between these two synclines with same orientation about 500m south of the site.

In the vicinity of the downstream-alternative site, good rock (CM class or better) occurs in the riverbed about 250m upstream of the site. However, outcropping of well argillized, D class rock is overall common at the site area. Furthermore, talus deposits are more widely distributed in comparison to the upstream site. Numerous float boulders are seen in the nearby creeks.

The geostructure of the downstream-alternative site comprises principally the St. Clair syncline which passes the left bank side of the Kotmale oya. An anticline is estimated to exist about 400m to the north of the site with NW-SE trending.

I.4.5.2 Results of Drilling and Seismic Prospecting

At the upstream-alternative for the P/S site (see LINE SL: CP-2-P, CP-2-C), the depth of occurrence of bed rock (CM class or better; excess of 2.2km/s) in the direction of the penstock route (Fig.-13) is 2~10m below the surface with the exception of GL-20m at survey points 70~130m and GL-

15~25m at survey points 560~660m. This reinforces the findings of site reconnaissance.

At survey points 610~650m, a portion of rock of low velocity (4.8km/s) in comparison to surrounding base rock in the vicinity (5.7~6.0km/s) is identified. This low velocity portion sits on the extended line from the lineament (an extremely marked lineament with the exception of the subject area) with N25°E trending determined from aerophotography. Judging from velocity, this portion is assumed to contain a certain amount of highly cracked rock (weakly weathered rock of CH class).

Rock of the site area consists principally of intermediate charnockite, interbedded with basic charnockite as seen at borehole CP-1 at GL-55~130m or intercalated with thin beds of felsic gneiss and granitic gneiss as seen at CC-1. The solid and broken lines in the figure represent extensions (estimated) of these formations, adopting dip and strike observed at the surface, with reference made to the boring core dip as well.

The cross-section which bisects the penstock route (LINE SL: CP-2-C) indicates base rock generally at a depth of GL-5~15m. However, at survey points 500~700m, base rock depth increases slightly to 15~25m.

The velocity for fresh rock in Fig. LINE SL: CP-2-P (the fifth layer in Table 5) shows some dispersion. The values for survey points 0~270m (4.9km/s) and 680~800m (5.2km/s) are somewhat smaller than those for points 270~680m (5.8~6.2km/s).

These low velocity zones represent points of intersection with the folding structures such as syncline and anticline, and are interpreted to signify zones of cracked or poor rock formed by folding.

The solid and broken lines in the figure indicate the granitic gneiss and alternation as described in i) above, and have been drawn with reference to the anticlinal axis at survey station 135m and the synclinal axis at 800m (see results of reconnaissance in 1 above).

At the downstream-alternative site for the power station (see LINE SL: CP-3-P, CP-3-C), the depth of bedrock (CM class or better) in the direction of the penstock route (LINE SL: CP-3-P) is GL-15~25m at survey

point 40~550m, and GL-6~15 at survey points 550~1030m. These depths are somewhat greater than those for the upstream-alternative site.

In this same cross section, low velocity zones (3.0~3.4km/s) are identified at survey points 60~80m, 250~260m, and 680~700m. Of these, that at points 60~80m is considered to be the same as that (2.8km/s) at points 60~70m in LINE SL: CP-3-P. Its orientation is assumed to be NNE-SSW. The orientation and continuity of the other low velocity zones could not be determined on the basis of data obtained.

I.4.6 Talawakelle Power Station Site

Both an upstream-alternative site and a downstream-alternative site are considered for the Talawakelle power station. The downstream-alternative site features both an underground alternative and a semiunderground alternative.

I.4.6.1 Results of Site Reconnaissance

(see attached route map FIG.I.4-7)

The geology of the overall Study area can be broadly classified into 3 formations: lower charnockite group, khondalite group, and upper charnockite group. At the subject site area, khondalite group and upper charnockite group are outcropped at the surface.

The boundary between these two formations is at 950m elevation for the upstream-alternative and at 1,000m for the downstream elevation. The upper charnockite group forms steep cliff, while the khondalite group comprises relatively gentle slope.

Large~small landslide zones are identified along the Kotmale oya and Pundal oya in the vicinity of the site. Of these, that along the left bank of the Pundal oya is considered to be landslide where stratification and slide plane coincide (this type exhibits slope surface failure), while that on both banks of the Kotmale oya consists primarily of clay originating from highly weathered khondalite.

The principal component of the geostructure of the site area is the Pundal oya syncline with NW-SE trending along the Pundal oya. Although the south wing of this syncline shows relatively stable strike and dip

(N20~60°W, 10~40°NE), the north wing displays extremely complex strike and dip fluctuation as a result of the effect of undulation with NW-SE trending axis. Overall, the syncline is considered to have slightly southward dip.

1.4.6.2 Results of Drilling and Seismic Prospecting

At the downstream-alternative site (see LINE SL: TP-2-P, TP-2-C, TP-3-C, TP-4-C, TP-5-C), bedrock along the penstock route (LINE SL: TP-2-P) is largely distributed at GL-3~10m, with the exception of the surgetank site and the cliff section (above TS-1). At the vicinity of the surgetank site, weathered rock (CL class) bed is 10~20m thick. Including the overlying talus deposits, baserock is located at GL-15~30m. Talus deposits are thickly distributed (maximum thickness: 25m) in the vicinity of boring no. TC-2.21, which is considered to be the results of said deposits filling a previously existing depression.

Rock is outcropped at the steep cliff section which exhibits marked vertical cracking. Rock is estimated to be CM~CH class (velocity of 3~4km/s).

At boring no. TS-1 and TP-22, Limonite (iron oxide) stain along crack planes is seen to about 45m depth, indicating oxidizing action of rainwater penetration.

As described in results of site reconnaissance above, rock in the site area is largely classified into two groups. Boring results further strongly support this conclusion. Stable rock facies of intermediate charnockite are found continuously distributed to the vicinity of GL-100m at boring no. TC-2.21, while irregular interbedding of intermediate charnockite, biotite gneiss, felsic gneiss, calc-gneiss, quartzite and crystalline limestone is in evidence at boreholes TS-1, TP-2 and TP-2'.

The solid line in the figure indicates an extension of characteristic beds or combination of beds determined through field survey and boring. Overall, the geostructure exhibits gentle undulation, with 5~10° dip towards the southeast.

Low velocity zones are identified in this cross-section at survey points 310~340m (3.5km/s), 445~450m (2.5km/s) and 590~600m (3.0km/s). Of

these, that at 310~340m is considered to possibly connect to the fault indicated on the Kotmale reservoir map.

In LINE SL: TP-3-C which intersects LINE SL: TP-2-P, distribution depth of baserock (CM class or better) is relatively shallow at GL-5~10m at survey points 0~1050m. Depth increases somewhat to GL-15~20m at points 1050~1400m.

Low velocity zones are numerous in this cross-section. Such zones are identified at survey points 320~330m (3.7km/s), 610~620m (2.9km/s), 670~685m (3.9km/s), 850~860m (3.3km/s), 1090~1100m (3.9km/s), 1200~1240m (3.7km/s) and 1290~1300m (3.0km/s). However, the trending of these low velocity zones could not be determined from surface geological survey.

The solid and broken lines in the figure indicate an extension of the formation in LINE SLI; TP-3-C with reference to the small fold structure seen on the surface.

Of the cross-sections intersecting LINE SL: TP-2-P, TP-5-C is the closest to Kotmale river. This area represents a land slide zone. With the exception of the interval between survey points 135~180m, outcropping of rock is seen in the ravine. Surface bed is considered to be 2~7m thick deposit of landslide debris.

Distribution depth of base rock in this cross-section is relatively shallow at GL-2~10m, and the boundary between this base rock and overlying clayey layer is anticipated as the slide dane..

The solid line in the figure is an extension of the rock classification in Fig-17. The formation within which landsliding occurs is easily weathered and argillized felsic gneiss. No significant low velocity zone was identified by seismic prospecting.

LINE SL; TP-4-C presents the results of seismic prospecting at the surge tank site. According to these results, distribution depth of base rock in this area is GL-5~10m at survey points 0~60m. However, at subsequent points, depth increases, reaching GL-20~25m at survey points 100~210m. At survey points 100~210m, base rock occurs at GL-10~15m. In this cross-section low velocity zones (2.2~2.4km/s) were identified at survey points 80~85m and 280~290m.

LINE SL: TP-5-C represents the cross-section passing under boring no. TP-2 and intersecting with LINE SL: TP-2-P. Base rock distribution

depth in this area is GL-5~15m. A low velocity zone (2.7km/s) is identified at survey points 115~130m.

The foregoing has presented a description of the geology at the various cross-sections occurring at the Talawakelle power station site. Overall, the base rock (B~A class) shows some dispersion of elastic wave velocity and is characterized by the presence of numerous low velocity zones. This fluctuation of base rock velocity values is considered to be the result of variations in intensify and trending of cracking.

Although the precise details of trending and features of low velocity zones was not clarified, these zones are considered to bear a relationship to the N20°E trending lineament identified through aerophotography and cracking and faulting with N20°E, N20~50°E, and E-W trend by field geological survey.

The downstream-alternative site for the power station (see LINE SL: TP-2-P) is situated in the vicinity of landslide zone. Landslide area can basically be divided into 2 zones, located respectively at survey points 440~1,140m and 1,170~1460m. As seen in LINE SL: TP-2-P debris is deposited at survey points 750~1,140m at 5~12m thickness. At the crest of landslide zone, debris layer is thin and depth of baserock is extremely shallow. On the other hand, debris is distributed in a 5~10m thick layer throughout the entire landslide area.

Distribution depth of base rock (CM class or better) on this LINE is GL-3~10m at the top of the steep slope at survey points 280~300m, and GL-0~5m at the base of the cliff at survey points 300~440m.

At the landslide zone, the depth of base rock is GL-3~15m at survey points 460~1,290m. However, moving downward, depth of base rock tends to increase to around GL-15~25m. At survey points 1,440~1,650, base rock depth is GL-10m. On the opposite bank at survey points 1,700~2,000m, depth is around GL-5~15m.

Numerous low velocity zones are identified, i.e. at survey points 50~60m (3.1km/s), 420~440m (3.0km/s), 560~570m (2.8km/s), 980~990m (2.8km/s), 1,120~1,130m (2.4km/s), 1,400~1,410m (3.2km/s), 1,750~1,770m (2.4km/s), 1,830~1,850m (2.9km/s). Several of these are considered to possibly correspond to faults indicated on the hazard map for Kotmale

reservoir. However, evidence to conclusively support this could not be obtained through the field survey.

LINE SL: TP-3-C is a cross-section intersecting LINE SL: TP-2-P and represents the cross-section for the crest of the landslide zone. The depth of rock in this section is extremely shallow at GL-1~3m. Base rock is distributed at GL-6~10m.

Three low velocity zones are identified i.e. at survey points 90~95m (2.6km/s), 190~195 (2.5km/s), 275~285m (2.7km/s).

I.5 Lugeon Test Results

Lugeon testing was conducted at each borehole at structure sites. Results are indicated in the Lugeon test sheet.

In this section, the Lugeon map prepared using the values obtained from the Lugeon test is discussed.

In the Project area, permeable layer is seen to considerable depth. This is considered as bearing relation to the lineament with N20°E trending, and crack and fault system with E-W trending identified in the area.

The following Lugeon values serve as criteria in determining suitable base rock for concrete dam.

| Lugeon value | Permeability | Treatment |
|--------------|----------------------------|----------------------------------|
| Lu > 30 | extremely highly permeable | removal and concrete replacement |
| 30 > Lu > 15 | highly permeable | low pressure grouting |
| 15 > Lu > 5 | less permeable | " |
| 5 > Lu | less impermeable | high pressure grouting |
| Lu = 0 | highly impermeable | no treatment required |

(1) Upstream-alternative Site for Caledonia Dam (see FIG. I.5-1)

In this cross-section, Lu > 30 extend to a maximum 25m depth on the right bank and to 3~8m on the left bank.

On the right bank above boring no. CD-4, 5 < Lu < 30 extends from 0~8m. However, at boring no. CD-3 along the sheared zone, the same value reaches somewhat deeper. Layer with this value is 3~8m thick on the left bank from the riverbed to EL 1360m. At CD-5 and CD-6, the layer extends wedge shape to deep layer. Below this is distributed an impermeable layer of Lu < 5. Nevertheless, at GL-30~40m at CD-5, 8 < Lu < 12 is obtained due to heavy cracking with dip of 45°, 60°, 70°, etc. Values within the Lu < 5 range were primarily Lu = 0.

(2) Downstream-alternative Site for Caledonia Dam (see FIG. I.5-2)

In this cross-section, the layer of Lu>30 is distributed above EL 1355m, and has a maximum thickness of 20m. There is a strong possibility that this layer extends to a deep level along the area believed to be an extension of the sheared zone at the right bank of the upstream-alternative site.

On the left bank, layer of Lu>30 is thought to be distributed in 0~6m thickness from around CD-12 up to EL 1355.

The layer of 5<Lu<15 occurs on the right bank below EL 1335m at thickness of 8~10m. However, along the aforescribed shear zone, the layer is believed to extend wedge shaped to somewhat deeper level.

On the left bank, the layer of 5<Lu<15 is distributed at 3~15m thickness above EL 1320. Above EL 1360, the thickness of the layer tends to increase.

These 5<Lu<15 layers are underlain by a layer of Lu<5. This low Lu layer is outcropped at the riverbed and the lower slopes on both banks. The values of the Lu<5 layer are almost all Lu=0; however, a value of Lu=8.2 is seen at CD-12 at GL-17~20m. This is considered the result of high angle open cracking of 70~80° (with slickenside) observed at the surface nearby.

(3) Caledonia Right Bank Profile (see FIG. I.5-3)

In this cross-section, classification is made into two layers of Lu>30 and Lu<5, respectively, the boundary of which is considered at EL 1315~1322.

(4) Caledonia Left Bank Profile (see FIG. I.5-4)

This cross-section is divided into three layers of Lu>15, 5<Lu<15 and Lu<5, respectively. Lu>15 is thought to extend from the surface to 5~10m depth. The layer of 5<Lu<15 is estimated to underlie this layer at 5~10m thickness and with lower boundary depth at EL 1290 (upstream of CD-5, this lower boundary depth is considered to be at somewhat higher elevation). At CD-5, 8<Lu<12 is recorded at GL-30~40m, and this is presumed to be the result of extensive cracking of 45~70° dip seen on the surface in the vicinity.

(5) Cross-section at CS-1~CS-4 (see FIG. I.5-5)

This cross-section is divided into two layers of Lu>30 and Lu<5, respectively. The Lu>30 layer is 15m thick in the vicinity of CS-4. Thickness increases, however, in the direction of CS-1, reaching 30~40m in some points. Also, a sheared zone is observed about midway between the two borings, along which it is considered possible that the Lu>30 layer extends to a deep level. At GL-30m at CS-4, 75<Lu<105 is recorded which is considered to be the result of heavy cracking of 45° and 80° dip seen on the surface.

(6) Saddle Profile (see IG. I.5-7)

The vicinity of CS-5 is divided into three layers of Lu>30, 15<Lu<30, and Lu<5, respectively. The layer of Lu>30 runs essentially parallel to the topography with thickness of 15~20m. Beneath this lies a layer of 15<Lu<30 which is 5~6m thick. In the vicinity of CS-1, this layer extends wedge shaped to deep level. This wedge shaped section corresponds to the direction of extension of the shear zone passing through the saddle. The Lu<5 layer is distributed at GL-20~25m roughly parallel to the ground surface.

In the vicinity of CS-6, ground is divided into two layers of Lu<30 and Lu>30, respectively. The Lu>30 layer is considered to be distributed in a bed 15~25m thick. Around the sheared zone which passes roughly 55m to the right of CS-6, the low Lu layer possibly extends to deep level. Also, a permeable layer of Lu=77 is seen at CS-6 at GL-12~16m. This is estimated to be the result of heavy cracking of 70~90° dip.

(7) Saddle Cross-section (see FIG. I-5-6)

At this cross-section, the Lu>30 layer is extremely thick at 25~45m. A sheared zone is present, and the said layer may partially extend to considerable depth.

At CS-3, the 5<Lu<15 layer is distributed in a bed 5~15m thick. As data is not available for CS-1 and CS-2, ground in these vicinities is expressed as Lu<30. The upper boundary of the Lu<5 layer is estimated at around GL-40 (EL. 1325m) at CS-3. However, on the left side of the cross-section, this boundary is anticipated at higher elevation.

(8) Landslide Profile (see FIG. I.5-8)

The Lu>30 layer in this cross-section is 20~25m thick, and is estimated to be distributed roughly parallel to the ground surface. However, a sheared zone is anticipated 55m to the right of CD-9, where the aforementioned layer is anticipated to possibly extend wedge-shaped to deep level.

(9) Talawakelle Dam Downstream Alternative Site (see FIG. I.5-9)

This cross-section is divided into three layers of Lu>30, 5<Lu<15 and Lu<5, respectively. The thickness of the Lu>30 layer is 6~8m at the riverbed, but thickens somewhat to 15~20m at the right bank slope. On the left bank, layer thickness is 15m. At TD-2 and TD-4, the Lu>30 layer extends wedge-shaped to around GL-20~30m. This is considered due to extensive cracking to deep level genetically related to the zone of repeating micro folding structures with N-S trending at the dam site.

The 5<Lu<15 layer is thinly distributed in a 3~4m thick bed extending from around EL 1215m on the right bank slope to the TD-1.

The upper boundary of the Lu<5 layer is at EL 1180m at the riverbed, and extends on both bank slopes roughly parallel to the ground surface.

(10) Talawakelle Dam Upstream-Alternative Site (see FIG. I.5-10)

This cross-section is divided into two layers of 30>Lu and 30<Lu, respectively. However, the boreholes TD-5 and TD-6 are located for their entire depth in the 30>Lu layer. The thickness of this layer is 20m at the riverbed and 40~45m at both bank slopes.

(11) Caledonia Power Station Upstream-Alternative Site (see FIG. I.5-11)

This cross-section is divided into four layers of Lu>30, 5<Lu<30, 5<Lu<15, and Lu<5. There is no sharp boundary between the 5<Lu<15 and 5<Lu<30 layers.

The Lu>30 layer has a thickness of 5~20m. Between CC-1 and CP-1, thickness of the layer shows a slight increasing trend to 10~20m thickness. At the upper portion of CC-1 and the lower portion of CP-1, thickness is less than 10m. However, values greater than Lu 30 were obtained at CC-1 at GL-30~40m and at CP-1 at GL-55~65m suggesting that the Lu>30 layer may extend wedge-like to deep level. Also, the 5<Lu<15

and $5 < Lu < 30$ layers are seen to underlie the $Lu > 30$ layer from around CC-1 to CP-1. Thickness of these layers is 5~10m, and as seen in the figure, they exhibit a tendency to extend wedge-shaped to deep level.

The upper boundary depth of the $Lu < 5$ layer is relatively shallow at the upper portion of CC-1 and at the lower portion CP-1 at GL-5~10m; however, depth increases to GL-10~30m from CC-1 to CP-1.

As seen at CP-1, $5 < Lu < 15$ is identified at GL-90~100m. It is highly possible that cracking is continuous to the surface.

Thus, layers of high Lu value to relatively deep level are present at the subject site. This is believed to be the effect of cracking accompanying the anticlinal axis running parallel to the river.

(12) Talawakelle Power Station Downstream-Alternative Site (see FIG. I.5-12)

At this cross-section, Lugeon test was conducted at 4 boreholes. As boreholes were well dispersed, a separate Lugeon map has been prepared for each hole.

At TC-2 and TC-2', ground is divided into two layers of $Lu < 30$ and $Lu < 5$, respectively. The boundary between these two layers was estimated on the basis of boring and seismic prospecting results.

However, as shown in the figure, the $Lu > 30$ layer is believed to extend wedge-shaped to deep level.

At the vicinity of TS-1, the $Lu > 30$ layer is estimated to be distributed largely to GL-30m, with one portion extending to GL-70m. At GL-93~110m at TS-1, a layer of $5 < Lu < 15$ is identified. There exists the possibility that high Lugeon value zone continues wedge-shaped to deep level.

A layer of $Lu > 30$ is distributed in a 8~15m thick bed at TP-2. One portion extends wedge shaped to below GL-70m. The underlying layer of $5 < Lu < 15$ is believed to be 5~15m thick, and is anticipated to extend to deep level along the aforescribed $Lu > 30$ layer wedge. At almost all boreholes, ground below GL-95m exhibits values of $Lu=0$; however, at some points, $0 < Lu < 5$ is seen.

At the vicinity of TP-2', ground is divided into two layers of $Lu > 30$ and $Lu < 5$ respectively. The boundary between these layers is

estimated to be at GL-5~15m. Also, at GL-35m at TP-2', a Lu=15 layer is identified.

I.6 Laboratory Testing

I.6.1 General

In the course of the subject Study, boring cores were subjected to laboratory testing.

Laboratory rock tests consisted of mechanical tests and physical properties tests. Test items are shown in the following table.

TABLE I.6-1 LABORATORY ROCK TEST

| Test item | Test quantity | | | | Total |
|--------------------------|--------------------|-----------------------|----------------------|----------------------|-------|
| | Caledonia dam site | Caledonia saddle site | Talawakelle dam site | Talawakelle P/S site | |
| Mechanical test | | | | | |
| Uniaxial | 28 | 15 | 10 | 16 | 699 |
| Triaxial | 5 | 1 | 1 | 2 | 9 |
| Tensile | 7 | 2 | 2 | 3 | 14 |
| Sonic | 6 | 2 | 2 | 2 | 12 |
| Physical properties test | | | | | |
| Bulk density | 50 | 26 | 15 | 25 | 116 |
| Porosity | 50 | 26 | 15 | 25 | 116 |
| Specific gravity | 50 | 26 | 15 | 25 | 116 |

In addition to the above, soundness test was performed utilizing the CQ-1 core samples.

Rock testing was carried out at the Pradeniya University soil mechanics laboratory. The results of testing were submitted to CECB in the "Upper Kotmale Project Rock Testing Report".

Test results are summarized in tables I.6-2~I.6-7.

TABLE I. 6-2

| Sample No. | Depth | Rock Classification | Bulk Specific gravity | | Effective porosity (%) | Unit Weight (g/cm ³) | Ultrasonic Velocity | | | | Unconfined Compression Strength (kg/cm ²) | Tangent Modulus of Static Elasticity (by Strain Gauge) x 10 ⁶ (kg/cm ²) | Static Poisson's ratio (by Strain Gauge) | Tensile Strength (kg/cm ²) | C. (kg/cm ²) | ∅ (degree) |
|------------|-------------|----------------------|-------------------------|-------------------------|-------------------------|----------------------------------|-----------------------------------------------------|------------------------------|----------------------------------------------------------------|-------------------------------|-------------------------------------------------------|------------------------------------------------------------------------------------------------|------------------------------------------|----------------------------------------|--------------------------|------------|
| | | | Natural | | | | Sonic Velocity Compre- ssional wave (km/s) | Transverse wave (km/s) | Young's modulus 10 ⁴ (kg/cm ²) | Dynamic Poisson's ratio | | | | | | |
| CD1a | 3.76~4.28 | Intermediate Ch. | 2.668 | 2.668 | 0.646 | 2.656 | | | | | 1,322.4 | 2.04 | | | | |
| CD2a | 17.91~18.31 | Intermediate Ch. | 2.697 | 2.697 | 0.526 | 2.687 | | | | | 1,530.0 | 1.00 | 0.27 | | | |
| CD2b | 18.99~20.41 | Biotite Gneiss | 3.055 | 3.055 | 0.423 | 3.046 | | | | | 1,456.6 | 1.84 | | | | |
| CD3a | 27.94~28.11 | Biotite Schist | 3.220 | 3.220 | 0.487 | 3.210 | | | | | 424.3 | 0.38 | 0.20 | | | |
| CD3b | 31.15~31.53 | Granitic Gneiss | 2.604 | 2.604 | 1.852 | 2.561 | | | | | 562.3 | 0.12 | 0.96 | | | |
| CD3c | 36.23~36.39 | Biotite Gneiss | 2.879 | 2.879 | 2.726 | 2.816 | | | | | 913.4 | 2.20 | | | | |
| CD3d | 39.27~39.53 | Granitic Gneiss | 2.611 | 2.611 | 0.700 | 2.597 | | | | | 628.6 | 0.80 | | | | |
| CD3e | 36.51~36.65 | Biotite Gneiss | 2.863 | 2.863 | 2.153 | 2.817 | | | | | | | | 39.5 | | |
| CD3f | 36.69~37.13 | Biotite Gneiss | 2.794 2.841 2.860 | 2.794 2.841 2.860 | 0.792 1.152 1.435 | 2.778 2.816 2.831 | | | | | | | | 34.5 | 184.0 | 50.1 |
| CD4a | 11.82~12.08 | Biotite Gneiss (S.W) | 3.264 | 3.264 | 0.288 | 3.257 | | | | | 2,027.3 | 1.24 | | | | |
| CD4b | 21.65~22.00 | Intermediate Ch. | 2.638 | 2.638 | 0.582 | 2.628 | | | | | 1,279.3 | 0.90 | | | | |
| CD4c | 22.48~22.75 | Intermediate Ch. | 2.657 | 2.657 | 0.503 | 2.647 | | | | | 669.8 | 0.86 | | | | |
| CD5a | 4.74~4.97 | Ch. (H.W) | 2.585 | 2.585 | 5.763 | 2.461 | 1.05 | 0.52 | 1.76 | 0.342 | 181.4 | 0.23 | | | | |
| CD5b | 7.38~7.67 | Intermediate Ch. | 2.654 | 2.654 | 0.518 | 2.645 | 2.49 | 1.55 | 15.2 | 0.184 | 1,534.3 | 3.56 | 0.33 | | | |
| CD5c | 7.91~8.43 | Intermediate Ch. | 2.701 2.690 2.679 | 2.701 2.690 2.679 | 0.703 1.155 0.806 | 2.686 2.665 2.665 | | | | | | | | 126.1 | — | — |
| CD5d | 14.40~14.60 | Biotite Schist | 3.279 | 3.279 | 0.965 | 3.253 | | | | | 883.4 | 1.91 | | | | |
| CD6a | 4.68~5.12 | Intermediate Ch. | 2.757 | 2.757 | 0.488 | 2.748 | | | | | 1,558.1 | 0.96 | | | | |
| CD6b | 9.34~9.50 | Biotite Gneiss | 2.927 | 2.927 | 1.302 | 2.896 | | | | | 1,314.4 | 1.44 | | | | |

TABLE I.6-3

| Sample No. | Depth | Rock Classification | Bulk Specific gravity | | Effective porosity (%) | Unit Weight (g/cm ³) | Ultrasonic Velocity | | | Unconfined Compression Strength (kg/cm ²) | Tangent Modulus of Static Elasticity (by Strain Gauge) x 10 ⁶ (kg/cm ²) | Static Poisson's ratio (by Strain Gauge) | Tensile Strength (kg/cm ²) | C. (kg/cm ²) | ∅ (degree) |
|------------|-------------|------------------------|-----------------------|--|------------------------|----------------------------------|---------------------------|------------------------|-------------------------------------------------------|-------------------------------------------------------|------------------------------------------------------------------------------------------------|------------------------------------------|----------------------------------------|--------------------------|------------|
| | | | Natural | | | | Compressional wave (km/s) | Transverse wave (km/s) | Young's modulus 10 ⁴ (kg/cm ²) | | | | | | |
| CD7a | 5.24~5.55 | Biotite Gneiss | 3.181 | | 0.442 | 3.171 | | | | 1,572.5 | 2.45 | 0.26 | | | |
| CD7b | 6.59~7.21 | Intermediate Ch. | 2.705 | | 2.478 | 2.654 | | | | | | | 87.8 | 53.3 | 65.5 |
| | | | 2.765 | | 1.424 | 2.735 | | | | | | | | | |
| | | | 2.693 | | 0.983 | 2.675 | | | | | | | | | |
| CD7c | 7.70~8.07 | Intermediate Ch. | 2.968 | | 0.408 | 2.960 | | | | 1,426.0 | 1.84 | | 109.9 | | |
| CD8a | 3.90~4.03 | Intermediate Ch. (W) | 2.691 | | 2.314 | 2.641 | 3.61 | 1.90 | 27.1 | | | | | | |
| CD8b | 7.71~8.05 | Intermediate Ch. (S.W) | 2.947 | | 0.298 | 2.941 | 7.09 | 4.06 | 129.5 | 1,647.2 | | | | | |
| CD8c | 9.90~10.21 | Felsic Gneiss | 2.457 | | 0.426 | 2.451 | | | | 1,424.0 | | | | | |
| CD9a | 23.00~23.18 | Intermediate Ch. (W) | 2.747 | | 6.330 | 2.607 | 3.11 | 1.64 | 18.8 | | | | | | |
| CD9b | 26.45~26.66 | Intermediate Ch. | 2.828 | | 0.501 | 2.817 | 5.90 | 3.23 | 77.3 | | | | | | |
| CD10a | 2.47~2.82 | Intermediate Ch. | 2.852 | | 0.744 | 2.836 | | | | 1,713.4 | 0.69 | | | | |
| CD10b | 3.52~3.94 | Intermediate Ch. | 2.801 | | 0.703 | 2.788 | | | | 1,646.8 | 0.54 | | | | |
| CD11a | 4.98~5.20 | Intermediate Ch. | 2.846 | | 1.869 | 2.830 | | | | 1,822.0 | 1.52 | 0.24 | | | |
| CD11b | 9.74~9.90 | Intermediate Ch. | 2.853 | | 1.992 | 2.803 | | | | 1,701.9 | 3.34 | | | | |
| CD12a | 4.18~4.55 | Intermediate Ch. (S.W) | 2.798 | | 0.450 | 2.790 | | | | 2,190.1 | 2.39 | | | | |
| CD12b | 6.98~7.50 | Intermediate Ch. | 2.848 | | 0.750 | 2.831 | | | | | | | 117.0 | 131.0 | 62.7 |
| | | | 2.847 | | 0.887 | 2.827 | | | | | | | | | |
| | | | 2.846 | | 0.907 | 2.828 | | | | | | | | | |
| CD12c | 7.70~8.01 | Intermediate Ch. | 2.842 | | 0.654 | 2.828 | | | | 1,889.0 | 1.79 | | 129.7 | | |
| CD12d | 8.94~9.27 | Intermediate Ch. | 2.853 | | 0.400 | 2.846 | | | | 2,076.7 | 4.29 | | | | |
| CD4Aa | 8.38~9.02 | Intermediate Ch. | 2.784 | | 0.412 | 2.776 | | | | 1,723.9 | 1.50 | 0.30 | | | |
| CD4Ab | 12.93~13.39 | Intermediate Ch. (S.W) | 2.809 | | 0.457 | 2.799 | | | | 1,450.5 | 1.50 | | | | |

TABLE I.6-4

| Sample No. | Depth | Rock Classification | Bulk Specific gravity | | Effective porosity (%) | Unit Weight (g/cm ³) | Ultrasonic Velocity | | | | Unconfined Compression Strength (kg/cm ²) | Tangent Modulus of Static Elasticity (by Strain Gauge) × 10 ⁶ (kg/cm ²) | Static Poisson's ratio (by Strain Gauge) | Tensile Strength (kg/cm ²) | C (kg/cm ²) | ∅ (degree) | |
|------------|-------------|------------------------|-----------------------|--|------------------------|----------------------------------|------------------------------------------|------------------------|-------------------------------------------------------|-------------------------|-------------------------------------------------------|------------------------------------------------------------------------------------------------|------------------------------------------|----------------------------------------|-------------------------|------------|--|
| | | | Natural | | | | Sonic Velocity Compressional wave (km/s) | Transverse wave (km/s) | Young's modulus 10 ⁴ (kg/cm ²) | Dynamic Poisson's ratio | | | | | | | |
| CD3f | 36.69~37.13 | Biotite Gneiss | 2.853 | | 1.479 | 2.820 | | | | | | | | | | | |
| CD5c | 7.91~8.43 | Intermediate Ch. | 2.694 | | 0.968 | 2.674 | | | | | | | | | | | |
| CD7b | 6.59~7.21 | Intermediate Ch. | 2.735 | | 1.663 | 2.701 | | | | | | | | | | | |
| CD7c | 7.70~8.07 | Intermediate Ch. | 2.733 | | 1.149 | 2.707 | | | | | | | | | | | |
| CD12b | 6.98~7.50 | Intermediate Ch. | 2.845 | | 0.520 | 2.833 | | | | | | | | | | | |
| CD12c | 7.70~8.01 | Intermediate Ch. | 2.851 | | 0.978 | 2.829 | | | | | | | | | | | |
| CS1a | 24.37~24.50 | Intermediate Ch. (H.W) | 2.857 | | 22.855 | 2.414 | 1.71 | 1.06 | 6.3 | 0.192 | | | | | | | |
| CS1b | 28.73~29.05 | Intermediate Ch. | 2.650 | | 0.983 | 2.633 | 5.81 | 3.20 | 64.3 | 0.281 | 1,194.8 | 1.20 | | | | | |
| CS2a | 11.60~11.76 | Felsic Gneiss | 2.789 | | 2.203 | 2.737 | | | | | 1,790.4 | 0.84 | 0.22 | 76.9 | 36.3 | 70.8 | |
| *CS2b | 13.65~14.15 | Felsic Gneiss | 2.813 | | 1.345 | 2.785 | | | | | | | | | | | |
| | | | 2.684 | | 1.242 | 2.662 | | | | | | | | | | | |
| | | | 2.879 | | 2.114 | 2.819 | | | | | | | | | | | |
| CS2c | 14.42~14.77 | Felsic Gneiss | 2.780 | | 2.341 | 2.737 | | | | | | | | 127.2 | | | |
| CS2d | 17.62~17.96 | Felsic Gneiss | 2.782 | | 0.796 | 2.767 | | | | | 844.4 | 0.70 | | | | | |
| CS3a | 22.12~22.34 | Felsic Gneiss (S.W) | 2.679 | | 0.961 | 2.658 | | | | | 1,031.3 | 0.82 | 0.25 | | | | |
| CS3b | 24.75~25.12 | Felsic Gneiss | 2.672 | | 1.134 | 2.614 | | | | | 1,373.2 | 0.71 | | | | | |
| CS4a | 12.40~12.90 | Intermediate Ch. | 2.777 | | 0.664 | 2.764 | | | | | 1,853.7 | 1.72 | | | | | |
| CS5a | 6.95~7.25 | Intermediate Ch. | 2.713 | | 0.459 | 2.705 | | | | | 1,806.2 | 1.45 | | | | | |
| CS6a | 11.99~12.35 | Biotite Gneiss | 3.137 | | 0.400 | 3.128 | | | | | 1,830.4 | 1.21 | | | | | |
| CS2b | 13.65~14.15 | Felsic Gneiss | 2.819 | | 1.565 | 2.788 | | | | | | | | | | | |

TABLE I.6-5

| Sample No. | Depth | Rock Classification | Bulk Specific gravity | | Effective porosity (%) | Unit Weight (g/cm ³) | Ultrasonic Velocity | | | Unconfined Compression Strength (kg/cm ²) | Tangent Modulus of Static Elasticity (by Strain Gauge) X 10 ⁶ (kg/cm ²) | Static Poisson's ratio (by Strain Gauge) | Tensile Strength (kg/cm ²) | C (kg/cm ²) | Ø (degree) |
|------------|-------------|------------------------|-----------------------|-------|------------------------|----------------------------------|---------------------------|-------------------------------------------------------|-------------------------|-------------------------------------------------------|------------------------------------------------------------------------------------------------|------------------------------------------|----------------------------------------|-------------------------|------------|
| | | | Natural | | | | Sonic Velocity | Young's modulus 10 ⁴ (kg/cm ²) | Dynamic Poisson's ratio | | | | | | |
| | | | | | | | Compressional wave (km/s) | Transverse wave (km/s) | | | | | | | |
| CQ1a | 1.87~2.11 | Intermediate Ch. | 2.732 | 2.732 | 0.643 | 2.720 | | | | 1,793.5 | 1.76 | | | | |
| CQ1b | 10.79~10.96 | Intermediate Ch. | 2.790 | 2.790 | 0.617 | 2.778 | | | | | | | | | |
| CQ1c | 24.64~24.97 | Intermediate Ch. | 2.869 | 2.869 | 0.553 | 2.858 | | | | 1,560.7 | 2.00 | 0.47 | | | |
| CQ1d | 31.83~32.05 | Pegmatite | 2.633 | 2.633 | 0.646 | 2.621 | | | | | | | | | |
| CQ1e | 38.26~38.60 | Granitic Gneiss | 2.680 | 2.680 | 0.365 | 2.673 | | | | 1,160.0 | 1.43 | | | | |
| CQ2a | 14.25~15.52 | Intermediate Ch. (W) | 2.760 | 2.760 | 1.445 | 2.729 | | | | | | | | | |
| CQ2b | 19.66~19.81 | Felsic Gneiss | 2.686 | 2.686 | 0.791 | 2.670 | | | | | | | | | |
| CQ2c | 28.92~29.36 | Felsic Gneiss | 2.989 | 2.989 | 0.566 | 2.977 | | | | 1,455.2 | 1.42 | | | | |
| CQ2d | 41.61~42.01 | | 2.728 | 2.728 | 0.716 | 2.713 | | | | | | | | | |
| CQ2e | 49.06~49.67 | | 2.849 | 2.849 | 0.671 | 2.835 | | | | 1,618.8 | 0.82 | | | | |
| CI1a | 21.70~21.87 | Intermediate Ch. (S.W) | 2.837 | 2.837 | 0.655 | 2.823 | | | | 1,719.3 | 1.86 | | | | |
| CI1b | 24.48~24.85 | Intermediate Ch. | 2.821 | 2.821 | 0.529 | 2.811 | | | | 1,790.0 | 1.40 | | | | |
| TD1a | 6.32~6.53 | Intermediate Ch. (S.W) | 2.71 | 2.71 | 1.02 | 2.689 | 5.16 | 3.20 | 66.3 | 1,123.4 | 1.42 | | | | |
| TD1b | 8.38~8.71 | Intermediate Ch. | 2.69 | 2.69 | 1.00 | 2.672 | 5.64 | 3.50 | 81.6 | 1,766.0 | 1.93 | | | | |
| TD2a | 5.00~5.31 | Intermediate Ch. | 2.61 | 2.61 | 0.60 | 2.603 | | | | 1,644.6 | 3.05 | | | | |
| TD3a | 10.90~11.28 | Intermediate Ch. (S.W) | 2.77 | 2.77 | 1.20 | 2.601 | | | | 1,286.5 | 0.99 | 0.21 | | | |
| *TD3b | 11.46~12.42 | Intermediate Ch. | 2.68 | 2.68 | 0.47 | 2.670 | | | | 1,246.1 | 0.79 | | 18.3 | 69.3 | |
| TD4a | 11.35~11.71 | Intermediate Ch. (S.W) | 2.78 | 2.78 | 0.55 | 2.767 | | | | 1,792.9 | 1.57 | 0.49 | | | |
| TD4b | 14.78~15.14 | Intermediate Ch. | 2.71 | 2.71 | 0.50 | 2.704 | | | | 1,539.5 | 8.29 | | | | |

TABLE I.6-6

| Sample No. | Depth | Rock Classification | Bulk Specific gravity | Effective porosity (%) | Unit Weight (g/cm ³) | Ultrasonic Velocity | | | Unconfined Compression Strength (kg/cm ²) | Tangent Modulus of Elasticity (by Strain Gauge) x 10 ⁶ (kg/cm ²) | Static Poisson's ratio (by Strain Gauge) | Tensile Strength (kg/cm ²) | C. (kg/cm ²) | ∅ (degree) |
|------------|---------------|------------------------------------|-------------------------|-------------------------|----------------------------------|----------------------------|-------------------------------------------------------|-------------------------|-------------------------------------------------------|-----------------------------------------------------------------------------------------|------------------------------------------|----------------------------------------|--------------------------|------------|
| | | | | | | Sonic Velocity | Young's modulus 10 ⁴ (kg/cm ²) | Dynamic Poisson's ratio | | | | | | |
| | | | Natural | | | Compre- sional wave (km/s) | Transverse wave (km/s) | | | | | | | |
| TD5a | 19.89~20.10 | Intermediate Ch. (H.W) | 2.99 | 4.40 | 2.878 | | | | 168.5 | 0.09 | | | | |
| TD5b | 27.43~27.69 | Basic Ch. (S.W) | 2.96 | 0.93 | 2.942 | | | | 1,275.0 | 2.08 | | | | |
| TD6a | 21.34~21.69 | Intermediate Ch. | 2.81 | 0.75 | 2.799 | | | | 1,047.9 | 0.84 | 0.17 | | | |
| TD3b | 11.46~12.42 | Intermediate Ch. (S.W) | 2.660 2.620 2.660 | 0.500 0.784 0.665 | 2.646 2.605 2.648 | | | | | | | | | |
| TD3b | 11.46~12.42 | - do - 3b (i) 3b (ii) | 2.680 2.690 | 1.569 1.917 | 2.646 2.655 | | | | | | | 55.4 85.1 | | |
| TS1a | 5.60~5.83 | Intermediate Ch. (W) | 2.900 | 3.98 | 2.801 | 2.80 | 1.44 | 14.5 | 530.4 | 0.13 | | | | |
| TS1b | 79.80~80.07 | Biotite Gneiss | 2.900 | 0.636 | 2.886 | | | | 1,418.2 | 1.50 | | | | |
| TS1c | 84.75~85.15 | Biotite Gneiss | 2.847 | 0.706 | 2.833 | 5.90 | 3.77 | 95.2 | 928.2 | 0.74 | 0.20 | | | |
| TS1d | 90.15~90.34 | Biotite Gneiss | 2.989 | 0.314 | 2.983 | | | | 1547.4 | 1.14 | | | | |
| TP2a | 221.15~221.41 | Felsic Gneiss | 2.890 | 1.571 | 2.856 | | | | 1,224.7 | 0.78 | | | | |
| TP2b | 230.22~230.58 | Felsic Gneiss | 2.809 | 0.557 | 2.805 | | | | 1,826.1 | 3.62 | | | | |
| TP2c | 240.01~240.40 | Quartzite | 2.971 | 0.513 | 2.959 | | | | 1,324.3 | 0.71 | | | | |
| TP2d | 250.38~250.85 | Intermediate Ch. | 2.883 | 1.723 | 2.850 | | | | 886.8 | 1.80 | | | | |
| TP2e | 260.01~260.43 | Intermediate Ch. | 2.769 | 0.672 | 2.754 | | | | 1,324.2 | 1.25 | | | | |
| TP2f | 270.16~270.64 | Felsic Gneiss | 3.076 | 0.701 | 3.059 | | | | 787.1 | 0.60 | 0.50 | | | |
| TP2g | 338.63~339.03 | Crystalline Limestone | 2.948 | 0.329 | 2.940 | | | | 952.0 | 0.67 | | | | |
| *TP2h | 246.16~247.06 | Felsic Gneiss~ Intermediate Ch. | 2.923 2.995 2.730 | 0.575 0.475 0.450 | 2.911 2.985 2.725 | | | | | | | (i) 53.24 (ii) 76.00 | | |

TABLE I.6-7

| Sample No. | Depth | Rock Classification | Bulk Specific gravity | | Effective porosity (%) | Unit Weight (g/cm ³) | Ultrasonic Velocity | | | Unconfined Compression Strength (kg/cm ²) | Tangent Modulus of Static Elasticity (by Strain Gauge) X 10 ⁶ (kg/cm ²) | Static Poisson's ratio (by Strain Gauge) | Tensile Strength (kg/cm ²) | C. (kg/cm ²) | Ø (degree) |
|------------|---------------|------------------------------------|-----------------------|--|------------------------|----------------------------------|-----------------------------------------------------|------------------------------|----------------------------------------------------------------|-------------------------------------------------------|------------------------------------------------------------------------------------------------|------------------------------------------|----------------------------------------|--------------------------|------------|
| | | | Natural | | | | Sonic Velocity Compre- ssional wave (km/s) | Transverse wave (km/s) | Young's modulus 10 ⁴ (kg/cm ²) | | | | | | |
| *TP2i | 339.03~339.98 | Crystalline Limestone | 2.917 | | 0.363 | 2.908 | | | | | | | 23.15 | 441.0 | 10.0 |
| TP2'a | 40.80~41.08 | Intermediate Ch. | 2.888 | | 0.299 | 2.881 | | | | | | | | | |
| TP2'b | 49.33~49.58 | Intermediate Ch. | 2.880 | | 0.244 | 2.874 | | | | | | | | | |
| TC2-2'a | 79.96~80.14 | Intermediate Ch. | 2.750 | | 1.110 | 2.732 | | | | 1,540.2 | 1.14 | 0.17 | | | |
| TC2-2'b | 84.75~85.02 | - do - | 2.740 | | 1.322 | 2.714 | | | | 1,296.9 | 0.94 | | | | |
| TC2-2'c | 89.97~90.19 | - do - | 2.777 | | 0.866 | 2.759 | | | | 1,523.7 | 2.08 | 0.27 | | | |
| TP2h (i) | 246.16~247.06 | Felsic Gneiss~ Intermediate Ch. | 2.783 | | 0.515 | 2.773 | | | | 1,616.6 | 1.70 | 0.39 | | | |
| TP2h (ii) | " " | - do - | 2.679 | | 0.436 | 2.670 | | | | 1,625.6 | 1.66 | | | | |
| TP2i (i) | 339.03~339.98 | Crystalline Limestone | 3.156 | | 1.000 | 3.090 | | | | | | | | | |
| | | | 2.770 | | 0.789 | 2.750 | | | | | | | | | |
| | | | 2.896 | | 0.300 | 2.889 | | | | | | | | | |

I.6.2 Unconfined Compressive Strength

The correlations between uniaxial compressive strength, unit weight, effective porosity and tangent modulus of static elasticity on a per site basis and an overall basis are shown in figures I.6-1~I.6-3. The figures present the said correlations by rock type.

(1) Unconfined compressive strength and unit weight

As shown in FIG. I.6-1, intermediate charnockite is somewhat concentrated within the broken line and exhibits a positive correlation for uniaxial compressive strength and bulk density. Although only a limited number of tests were run for biotite gneiss, it exhibited a positive correlation. Test samples for other types of rock were few and no marked concentration was seen; however, felsic gneiss tended to concentrate within the broken line.

Compressive strength for intermediate charnockite ranged from 1000kgf/cm² ~ 1900kgf/cm², with values concentrated at 1500~1800kgf/cm². Bulk density ranged from 2.50~2.75g/cm³.

In comparison with intermediate charnockite, basic charnockite exhibits somewhat greater bulk density at 2.75~3.05g/cm³.

Biotite schist showed values of 3.20~3.25g/cm³ for density and 400; 900kgf/cm² for compressive strength. Quartzite exhibited values of 2.85g/cm³ and 1300kg/cm², respectively, for the same. The respective values for crystalline limestone were 2.85g/cm³ and 950kgf/m².

(2) Uniaxial compressive strength and porosity

As seen in FIG. I.6-2, there is no correlation between compressive strength and porosity.

Porosity for intermediate charnockite, biotite gneiss, felsic gneiss, granitic gneiss, quartzite, and crystalline limestone tend to concentrate around 0.3~0.7%. Nevertheless there were numerous examples where values were in excess of this range. One portion of felsic gneiss showed values higher than other types of rock at 0.7~2.2%. Also, one portion of intermediate charnockite yielded porosity values at 1.9~2.0% despite compressive strength of 1700~1800.

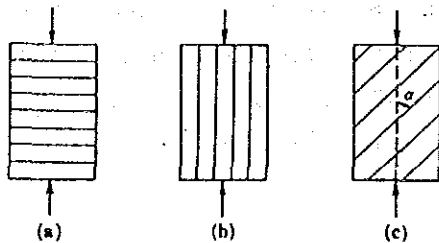
On a per site basis, values at the Caledonia dam site showed somewhat concentration at 0.4~0.5%; while at other sites no significant concentration was seen.

(3) Uniaxial compressive strength and tangent modulus of elasticity

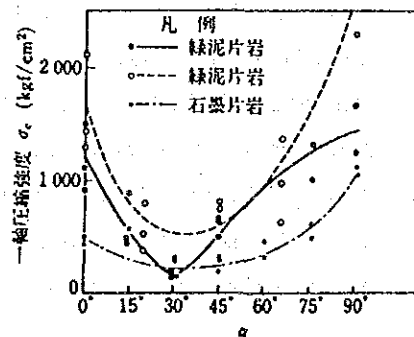
In FIG. I.6-3, a slight concentration is seen around the broken line. An overall positive correlation between uniaxial compressive strength and tangent modulus of elasticity is evidenced. No significant difference is noted by rock type, with values being mainly plotted along the broken line. Most tangent moduli of elasticity are concentrated at $0.6\sim 2.0 \times 10^6 \text{kgf/cm}^2$.

On a per site basis, a slight concentration of values around the broken line is seen for the Talawakelle dam and power station sites. For other sites, however, values are dispersed.

The above discussion has presented the correlation between compressive strength and physical properties, and compressive strength and deformation characteristics. In testing, compressive strength exhibits a strong relationship with rock anisotropy, in other words discontinuous surfaces such as stratification, schists and joints, etc. When load direction, and stratification and schistosity are in a relationship as shown in FIG. I.6-4, change in compressive strength occurs as shown in FIG. I.6-4. Compressive strength is at a minimum when the angle between load direction, and bedding and schist planes is around 30° . Under these conditions, elasticity modulus and compressive strength drop to around $60\sim 80^\circ$ in comparison to a load direction ~ bedding/schist plane angle of 90° where such bedding and or schistosity has no effect.



Relation between Load Direction and Bedding Layer



Unconfined Compression Strength v.s. Schistosity Degree

Within the study area, load conditions of this type exist at the Caledonia dam site and the Caledonia saddle. However, a trend as shown in the above figure is not seen. This is due to the difference between schistosity and gneissosity. Core examination revealed the presence of numerous cracks with slickenslide along the gneissosity, resulting in weak lines at the boundary of lithofacies.

In the case of hard rock, there are instances where rock of different character is intercalated in seam-like form. In the subject Study, the CD-4 sample is of this type, exhibiting a 2cm wide mafic band intercalated in charnockite. The strength of this sample is considered as governed by the strength of the mafic band and the strength of the boundary between the mafic band and the charnockite. In the case of this sample, failure occurs along the said boundary, and a low strength value of 670kgf/cm² is obtained. Slickenside is generally seen on this type of boundary surface, and it is referred to as a foliation joint or foliation shear.

In this manner, such discontinuous surfaces such as bedding planes, etc. result in marked anisotropy in strength characteristics of foundation rock.

Furthermore, a large variation in compressive strength results depending on the degree of weathering cracking of rock.

Low strength values of 880kgf/cm² for biotite schist and 180kgf/cm² for highly weathered charnockite were obtained.

I.6.3 Triaxial Compressive Strength

A total of nine series of triaxial compressive strength tests were conducted. Of these, fracture strength dropped as cell pressure was increased. As a result, shear strength could not be determined.

Results of triaxial compressive strength test are shown in Table I.6-8.

TABLE 1.6-8 TRIAXIAL COMPRESSIVE TEST RESULTS

| Test No. | Depth (m) | Rock type | Cfg/m ² | φ (°) |
|----------|---------------|--------------------------|--------------------|-------|
| CD-3f | 36.69~37.13 | Biotite gneiss | 184.0 | 50.1 |
| CD-7b | 6.59~7.21 | Intermediate Charnockite | 53.3 | 65.5 |
| CD-12b | 6.98~7.50 | Intermediate Charnockite | 131.0 | 62.7 |
| CS-2b | 13.65~14.15 | Felsic gneiss | 36.3 | 70.8 |
| TD-3b | 11.46~12.42 | Intermediate Charnockite | 18.3 | 69.3 |
| TP-2i | 339.03~339.98 | Crystalline limestone | 441.0 | 10.0 |

As seen in the above table, C, φ show considerably dispersed values. This is considered as the result of the previously discussed rock anisotropy. The Mohr's circle determining C and φ are shown in figures I.6-5.

I.6.4 Tensile Strength Test

A total of 14 series of tensile strength tests were conducted. Results are shown in the following table.

According to these results, intermediate charnockite mostly shows values in excess of 85kgf/cm². For the slightly weathered sample, however, a somewhat small value of 55kgf/cm² was obtained. Felsic gneiss showed values in excess of 75kgf/cm². In contrast, biotite gneiss exhibited values at 35~40kgf/cm², which are low in comparison to those for other types of rock. Although mode of failure is not clear, low values for biotite gneiss are estimated to be the result of failure along biotite lamella (gneissosity). Crystalline limestone showed the lowest tensile strength at 23kgf/cm².

I.6.5 Sonic Test

Sonic testing was conducted on a total of 12 samples.

Results are as shown in Table I.6-10. These samples were taken primarily to determine speed resulting from varying degrees of weathering.

According to these results, fresh intermediate charnockite exhibits a vertical wave velocity generally in excess of 5.6km/s or more. However,

TABLE 1.6-9 TENSILE STRENGTH TEST RESULTS

| Test No. | Depth (m) | Rock type | Tensile strength (kgf/cm ²) |
|-----------------|---------------|------------------------------------------|-----------------------------------------|
| CD-3e | 36.51~36.65 | Biotite gneiss | 39.5 |
| CD-3f | 36.69~37.13 | Biotite gneiss | 34.5 |
| CD-5c | 7.91~8.43 | Intermediate Charnockite | 126.1 |
| CD-7b | 6.59~7.21 | Intermediate Charnockite | 87.8 |
| CD-7c | 7.70~8.07 | Intermediate Charnockite | 109.9 |
| CD-12b | 6.98~7.50 | Intermediate Charnockite | 117.0 |
| CD-12c | 7.70~8.01 | Intermediate Charnockite | 129.7 |
| CS-2b | 13.65~14.15 | Felsic gneiss | 76.9 |
| CS-2c | 14.42~14.77 | Felsic gneiss | 127.2 |
| TD-3b (i) (SW) | 11.46~12.42 | Intermediate Charnockite | 55.4 |
| TD-3b (ii) (SW) | 11.46~12.42 | Intermediate Charnockite | 85.1 |
| TP-2h(i) | 246.16~247.06 | Felsic gneiss ~ intermediate Charnockite | 53.24 |
| TP-2h(ii) | 246.16~247.06 | Felsic gneiss ~ intermediate Charnockite | 76.00 |
| TP-2i | 339.03~339.98 | Crystalline limestone | 23.15 |

the CD-5b sample yielded a value of 2.5km/s. Judging from physical properties and values for uniaxial compressive strength, this is concluded to be an error in measurement.

For slightly weathered rock, values of 5.2km/s and 7.1km/s were obtained. The 5.2k/s value is concluded to reflect variation in degree of weathering.

Weathered rock showed values of 2.8~3.6km/s, while highly weathered rock produced a value of 1.0~1.7km/s. The range of values in each case is considered to indicate slight variations of degree of weathering within the assigned category. However, in the case of highly weathered rock there were instances where sampling was not possible due to heavy argillization. These argillized zones were assumed to have velocity values of 0.5~0.7km/s.

Although the sonic test is performed on a single sample core, such cores in reality often represent block formations bordered by cracking. In other words, the results of sonic testing must be considered separately from seismic prospecting.

TABLE I.6-10 ULTRASONIC TEST RESULTS

| Test No. | Depth (m) | Rock type | Sonic wave velocity | |
|----------|-------------|-------------------------------|----------------------|------------------------|
| | | | Vertical wave (km/s) | Horizontal wave (km/s) |
| CD-5a | 4.74~4.97 | Charnockite (HW) | 1.05 | 0.52 |
| CD-5b | 7.38~7.67 | Intermediate charnockite (F) | 2.49 | 1.55 |
| CD-8a | 3.90~4.03 | Intermediate charnockite (W) | 3.61 | 1.90 |
| CD-8b | 7.71~8.05 | Intermediate charnockite (SW) | 7.09 | 4.06 |
| CD-9a | 23.00~23.18 | Intermediate charnockite (W) | 3.11 | 1.64 |
| CD-9b | 26.45~26.66 | Intermediate charnockite (F) | 5.90 | 3.23 |
| CS-1a | 24.37~24.50 | Intermediate charnockite (HW) | 1.71 | 1.06 |
| CS-1b | 28.73~29.05 | Intermediate charnockite | 5.81 | 3.20 |
| TD-1a | 6.32~6.53 | Intermediate charnockite (SW) | 5.16 | 3.20 |
| TD-1b | 8.38~8.71 | Intermediate charnockite | 5.64 | 3.50 |
| TS-1a | 5.60~5.83 | Intermediate charnockite (W) | 2.80 | 1.44 |
| TS-1c | 84.75~85.15 | Biotite gneiss | 5.90 | 3.77 |

W: weathered
 HW: highly weathered
 SW: slightly weathered
 F: fresh rock

I.6.6 Physical Tests

Physical property testing consisted of specific gravity, porosity and bulk density tests. Specifics of the results of these tests have been discussed in the previous section I.6.1.

I.7 Site Evaluation

Hereinunder, each site will be evaluated and problem points identified.

I.7.1 Caledonia Dam Area

Both an upstream and downstream-alternative site are considered for Caledonia dam.

Although outcropping of rock is favorable at the downstream site, there is a relatively large landslide zone on the right bank immediately upstream of the site. Also, a fault with N60°E trending is identified on the right bank abut.

In the case of the upstream-alternative site, a portion of landslide zone is present at the right bank abut, and the bed of highly weathered rock on the right bank reaches 15m in thickness. As a result, a large amount of excavation would be necessary.

A common problem affecting both alternative sites is the possibility that the low velocity zone identified on the right bank runs parallel to the river. This type of low velocity zone is often a source of seepage and piping following ponding. As a result, further detailed survey of the low velocity zone is necessary. Detailed survey is also required to determine the extent of cracking accompanying the anticline structure passing along the river bed.

I.7.2 Caledonia Dam Saddle Area

Overall, weathering in this area extends to deep level. At points, thickness of the highly weathered bed reaches 30m. A fault with trending N50°W is estimated to pass through the saddle. Also, a fault with N35°E trending is believed to extend from upstream of the dam site to the saddle. If this faulting is accompanied by fracture zones, there exists the possibility of seepage. Under such conditions, placement of a diaphragm in the base rock (CM class or better) would be effective.

Results of boring at the saddle indicate extensive cracking, which would require appropriate grouting measures.

I.7.3 Talawakelle Intake Dam Area

Both an upstream and downstream-alternative site were considered for the Talawakelle dam site. However, the upstream site is distributed with weathered rock under the river bed to a depth of about 13m. An unclear low velocity zone is also identified at the river bed. On the basis of these factors, the upstream site is considered inappropriate for dam construction.

At the downstream site, outcropping of rock occurs at the riverbed. Dam height is low, and minimal problems in construction are anticipated. However, bed of weathered rock on both banks is 10~15m thick, and appropriate foundation treatment at abuts will be necessary.

I.7.4 Caledonia Power Station Area

Both an upstream and downstream-alternative site were initially considered for the Caledonia Power Station site. However, the downstream-alternative was subsequently abandoned on the basis of structural problems affecting the envisioned facilities. An underground power station is planned at the upstream site.

At the upstream site, depth of base rock is relatively shallow. Boring indicates the presence of hard and compact rock. Surface survey identified an anticline with NW-SE trending about 500m south of the site. As there exists the possibility that cracking and weathering extend to deep level in the vicinity of the anticline, as well as the fact that the Lugeon map for the area shows high Lugeon value zones in deep ground, it is proposed that the power station site be located as far from the anticline as possible. Accordingly, the candidate site has been moved a further 250m downstream close to the syncline axis.

Seismic prospecting identified a low velocity zone on the right bank of the Kotmale oya. Nevertheless, judging from the velocity value, rock is believed to be CH class. Accordingly, no structural problems are anticipated.

On the other hand, in comparison to the upstream site, the downstream site has relatively thick bed of highly weathered rock. Baserock occurs at GL-10~25m. Seismic prospecting identified the

occurrence of 3~4 low velocity zones. As a result, the downstream-alternative is considered inappropriate as a structure site.

I.7.5 Talawakelle Power Station Area

Both an upstream and downstream site are considered for the Talawakelle power station site. An underground power station is proposed for the upstream site, while at the downstream site both an underground alternative and a semi-underground alternative were studied.

The upstream site is located in a large landslide zone area which adversely affects the surface switchyard and control room structures. Furthermore, the underground power station is located in ground where strike and dip (dip in the direction of the Pundal oya) are such that the structure could be anticipated to be subjected to higher ground stress from the mountain side (southeast side). On the basis of these factors, the upstream-alternative is considered inappropriate.

At the downstream site, seepage of meteoric water to a depth of 45m is in evidence. However, below that, good rock is distributed. Furthermore, as the geostructure is basically level, the possibility of unbalanced ground stress as mentioned above is small. As a result, construction of an underground power station is considered feasible.

On the other hand, the semi-underground alternative site is located in an area of landslide zone, with significant low velocity zone to the immediate east (the presence of a fault as seen at the upstream site is possible). Consequently, appropriate countermeasures for these conditions would be necessary during construction. On the basis of the foregoing, the underground proposal is considered to be the more technically feasible.

However, seismic prospecting has identified numerous low velocity zones in the area, and judging from their orientation, some could be expected to intersect the penstock route. Also, the underground power station would be constructed in khondalite group, which due to its generally banded structure can often cause rock fall, etc. by foliation resulting from stress release.

The relative relief of the area is extremely large. Slippage of large-scale blocks often occurs in such an area. However, there are cases

where blocks are so large that they exceed beyond the physical area covered of detailed survey. At points of sharp topographical change, such as the boundary between level area and steep slope at the surge tank site, seismic prospecting and where necessary trench survey should be conducted to clarify degree of geologic discontinuity or faulting along the sharp topographical change.

1.7.6 Tunnel Routes

A surface geologic survey was conducted to gather geologic data along the envisaged Caledonia headrace and tailrace tunnels and the Talawakelle headrace tunnel.

Geologic data considered important in tunnel design and construction include rock classification, rock strength, degree of weathering, thickness of overburden, extent and trending of cracking, geostructure (presence of faulting and fold structures), etc.

In the case of the subject Project area where base rock must have adequate strength, degree of weathering of rock and conditions of geostructure are particularly important. Specifically, in regards to weathering, weathering at the tunnel shaft entrance, weathering where overburden is thin, and weathering at deep level (in association with faulting or concentrated cracking) are potential problems. In the case of geostructure, heavy water outpour at deep level, swelling of fault clay, ground stress at fold structures and concentration of cracking would be conditions posing potential problems.

Caledonia Headrace and Tailrace Tunnels

In the vicinity of the Caledonia dam site, tunnel passes through charnockite. In the vicinity of the power station, tunnel route passes through khondalite group (alternation of charnockite, felsic gneiss, biotite gneiss, etc.). Charnockite is generally relatively massive. In contrast, khondalite exhibits clearly banded structure, and the possibility is considered great for heavy weathering in the vicinity of the fold structure, particularly the anticlinal axis, and the lineament.

However, as the tunnel route is planned along the St. Clair syncline, geostructurally good rock with less cracking is anticipated.

Nevertheless, two faults trending NNE-SSW and NE-SW at the Caledonia dam site, a marked lineament of NNW-SSE trending at the Caledonia power station site, and lineament of NE-SW trending at the midway portion of the tailrace tunnel have been identified. These lineaments are observed as sheared zones with almost no displacement. However, judging from overall weathering, possibility is considered high that lineaments serve as corridors for meteoric and ground water. During excavation, careful attention will have to be given the degree of water outpour and rock weathering.

Talawakelle Headrace Tunnel (see FIG.I.7-1)

The Talawakelle headrace tunnel is 13km long. In comparison with the Caledonia headrace and tailrace tunnels, tunnel route must pass through numerous fold axes and lineaments. As a result, a long time period would be necessary for excavation.

FIG.I.7-1 presents a cross-section along the tunnel route axis prepared on the basis of surface survey and test boring.

According to the cross-section, the tunnel route for 3.4km from the Talawakelle intake (tunnel starting point) passes through lower charnockite group. From the 3.4km point to the 6.1km point, the route is through khondalite group, and from point 6.1km to the surge chamber, the route passes through upper charnockite group.

Geostructurally, the tunnel crosses the Saint Clair syncline at the 0.8km point, and the Belton-Meddecombra anticline at the 2km point. Between these two folding axes, minor anticline (1,030m point) and syncline (1,500m point) with identical trending are found. However, the tunnel interval from starting point to the 2km point corresponds to the Talakawelle structural bend zone, and the major folding structure becomes somewhat unclear.

In this section, cracking accompanying minor folding with N-S trending, and the NE-SW crack system oblique to the major folding are not marked. However, there is possibility of weathered zone and heavy water outpour at the anticlinal axis.

For the 8.7km interval from the Belton-Meddecombra anticline to the Pundal oya syncline, ground dips gently to the northeast, and good rock is anticipated in the kondalite group and upper charnockite group. However,

care must be given the fact that overburden at the 4.4km point is around 800m which may cause rock burst especially in massive compact rock.

After passing Pundal oya, the tunnel route turns to the northwest and proceeds roughly parallel to the Pundal oya syncline. Although this part of the route intersects numerous lineaments, i.e. at the 9.2km point (NNE-SSW trending), the 10km point (N-S trending), 11.35km point (NNE-SSW trending), and 12.3km point (E-W trending), geostructural condition is stable. Nevertheless, during excavation at these points, care must be given to weathered zones and seepage.

FIGURES

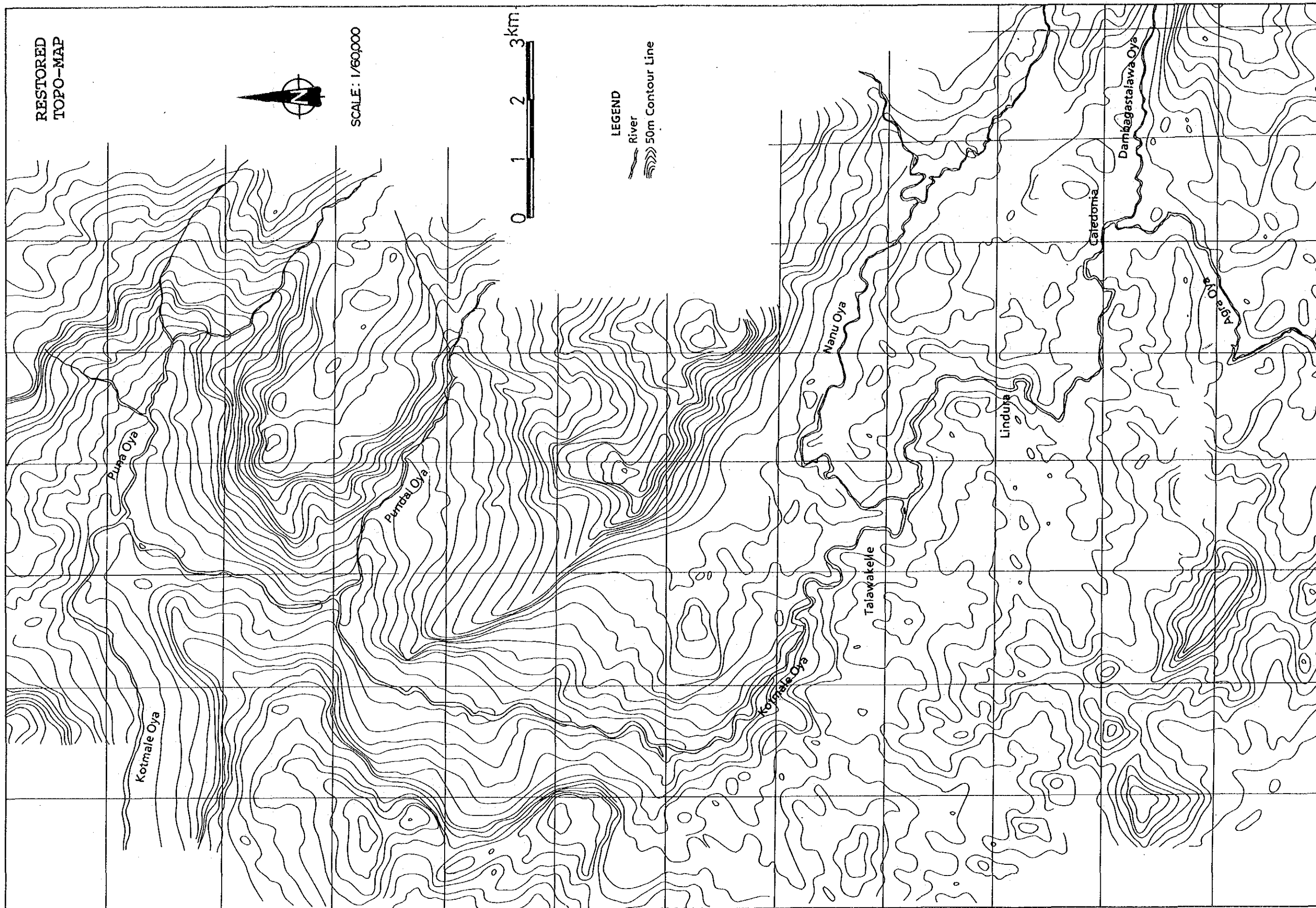
List of Illustrations

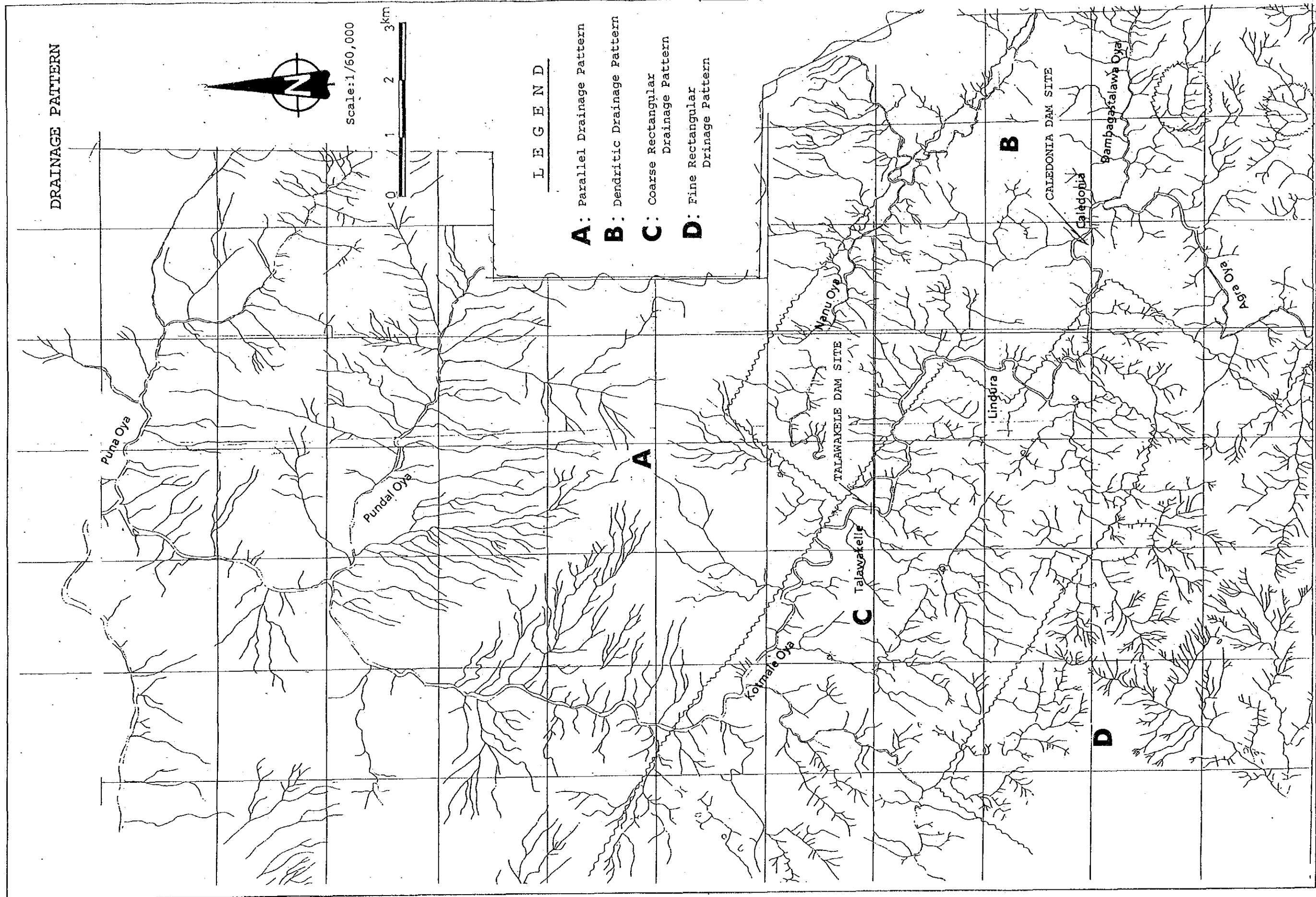
| | <u>Page</u> |
|----------------------------------------------------------------------------------------|-------------|
| FIG. I.1-1 Restored Topo-map | I-F-1 |
| I.1-2 Drainage Pattern | I-F-2 |
| I.1-3 Relative Relief Map | I-F-3 |
| I.2-1 Drilling Site and Seismic Prospecting Line for Caledonia Dam Area | I-F-4 |
| I.2-2 Drilling Site and Seismic Prospecting Line for Talawakelle Dam Area | I-F-5 |
| I.2-3 Drilling Site and Seismic Prospecting Line for Caledonia P/S Area | I-F-6 |
| I.2-4 Drilling Site and Seismic Prospecting Line for Talawakelle P/S Area | I-F-7 |
| I.2-5 Seismic Prospecting Line for Talawakelle P/S Upstream-alternative | I-F-8 |
| I.4-1 Geological Route Map | I-F-9 |
| I.4-2 Geological Structure Map | I-F-10 |
| Legend for Geological Maps | I-F-11 |
| I.4-3 Geological Map for Caledonia Dam Area | I-F-12 |
| I.4-4 Geological Map for Caledonia Reservoir Area | I-F-13 |
| I.4-5 Geological Map for Talawakelle Dam Area | I-F-14 |
| I.4-6 Geological Map for Caledonia P/S Area | I-F-15 |
| I.4-7 Geological Map for Talawakelle P/S Area | I-F-16 |
| Legend for Geological Sections | I-F-17 |
| I.4-8 Geological Section for Seismic Line SL: CD-1 | I-F-18 |
| I.4-9 Geological Section for Seismic Line SL: CD-2 | I-F-19 |
| I.4-10 Geological Section for Seismic Line SL: CD-3 | I-F-19 |
| I.4-11 Geological Section for Seismic Line SL: CD-4 | I-F-20 |

| | <u>Page</u> |
|-----------------------------------------------------------------|-------------|
| I.4-12 Geological Section for Seismic Line SL: CD-5 | I-F-20 |
| I.4-13 Geological Section for Seismic Line SL: CD-6 | I-F-21 |
| I.4-14 Geological Section for Seismic Line SL: CD-7 | I-F-21 |
| I.4-15 Geological Section for Seismic Line SL: CD-8 | I-F-22 |
| I.4-16 Geological Section for Seismic Line SL: CD-9 | I-F-22 |
| I.4-17 Geological Section for Seismic Line SL: CD-10 | I-F-23 |
| I.4-18 Geological Section for Seismic Line SL: TD-1 | I-F-24 |
| I.4-19 Geological Section for Seismic Line SL: DD-2 | I-F-24 |
| I.4-20 Geological Section for Seismic Line SL: CP-2-P | I-F-25 |
| I.4-21 Geological Section for Seismic Line SL: CP-2-C | I-F-26 |
| I.4-22 Geological Section for Seismic Line SL: CP-3-P | I-F-27 |
| I.4-23 Geological Section for Seismic Line SL: CP-3-C | I-F-27 |
| I.4-24 Geological Section for Seismic Line SL: TP-2-P | I-F-28 |
| I.4-25 Geological Section for Seismic Line SL: TP-2-C | I-F-29 |
| I.4-26 Geological Section for Seismic Line SL: TP-3-C | I-F-30 |
| I.4-27 Geological Section for Seismic Line SL: TP-4-C | I-F-31 |
| I.4-28 Geological Section for Seismic Line SL: TP-5-C | I-F-32 |
| I.4-29 Geological Section for Seismic Line SL: TP-1-P | I-F-33 |
| I.4-30 Geological Section for Seismic Line SL: TP-1-C | I-F-33 |
| I.5-1 Lugeon Map for SL: CD-1 | I-F-34 |
| I.5-2 Lugeon Map for SL: CD-2 | I-F-35 |
| I.5-3 Lugeon Map for SL: CD-3 | I-F-35 |
| I.5-4 Lugeon Map for SL: CD-4 | I-F-36 |
| I.5-5 Lugeon Map for SL: CD-5 | I-F-36 |
| I.5-6 Lugeon Map for SL: CD-6 | I-F-37 |
| I.5-7 Lugeon Map for SL: CD-8 | I-F-38 |
| I.5-8 Lugeon Map for SL: CD-9 | I-F-38 |

| | <u>Page</u> |
|------------------------------------------------------------------------------------------------|-------------|
| I.5-9 Lugeon Map for SL: TD-1 | I-F-39 |
| I.5-10 Lugeon Map for SL: TD-2 | I-F-39 |
| I.5-11 Lugeon Map for SL: CP-2-P | I-F-40 |
| I.5-12 Lugeon Map for SL: TP-2-P | I-F-41 |
| I.6-1 Unconfined Compressive Strength versus Unit Weight | I-F-42 |
| I.6-2 Unconfined Compressive Strength versus Effective Porosity | I-F-45 |
| I.6-3 Unconfined Compressive Strength versus Tangent Modulus of Static Elasticity | I-F-48 |
| I.6-4 Triaxial Compression Test Data | I-F-51 |
| I.7-1 Geological Profile for Talawakelle Headrace Tunnel | I-F-55 |

FIG. I.1-1





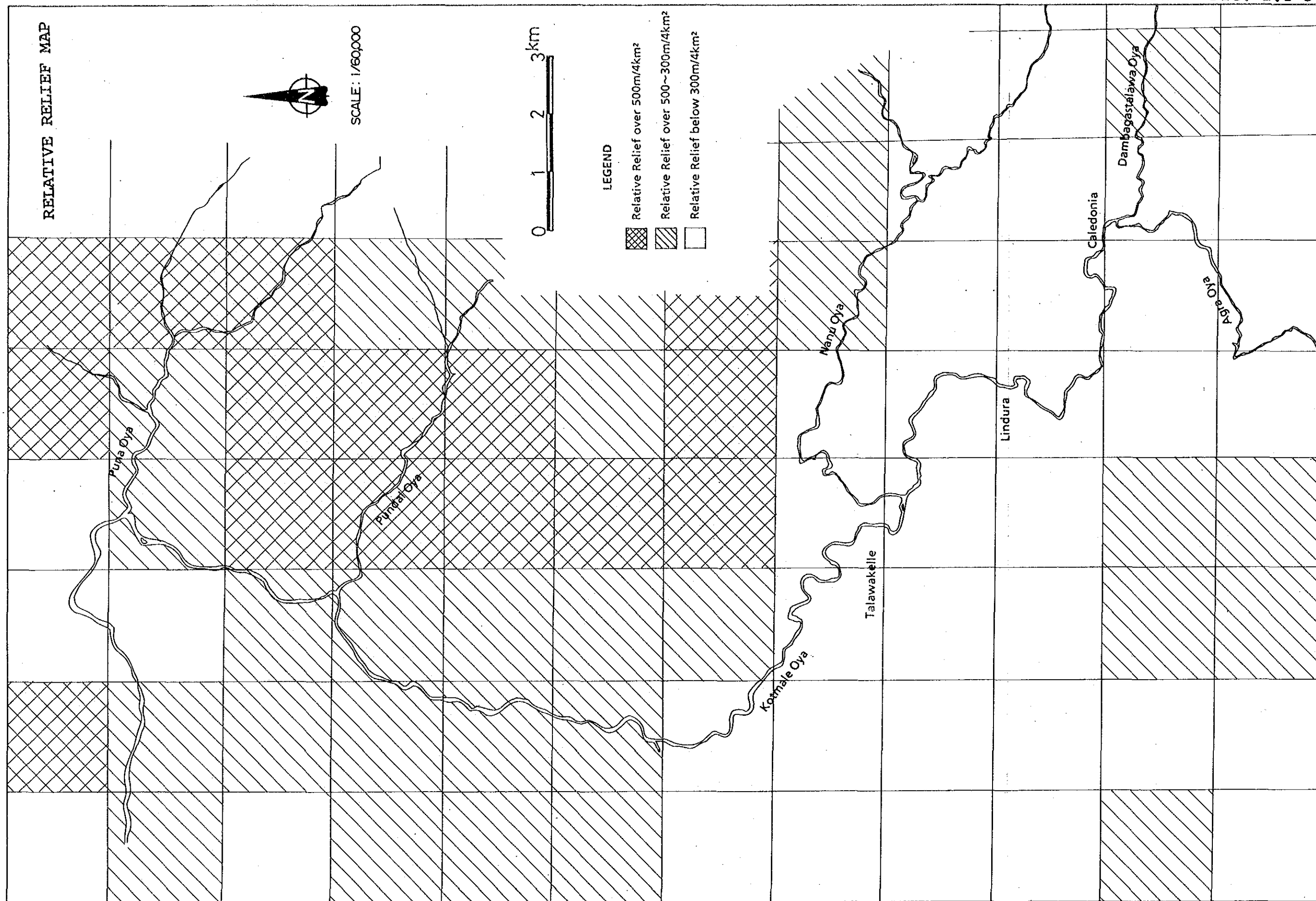


FIG. I.2-1

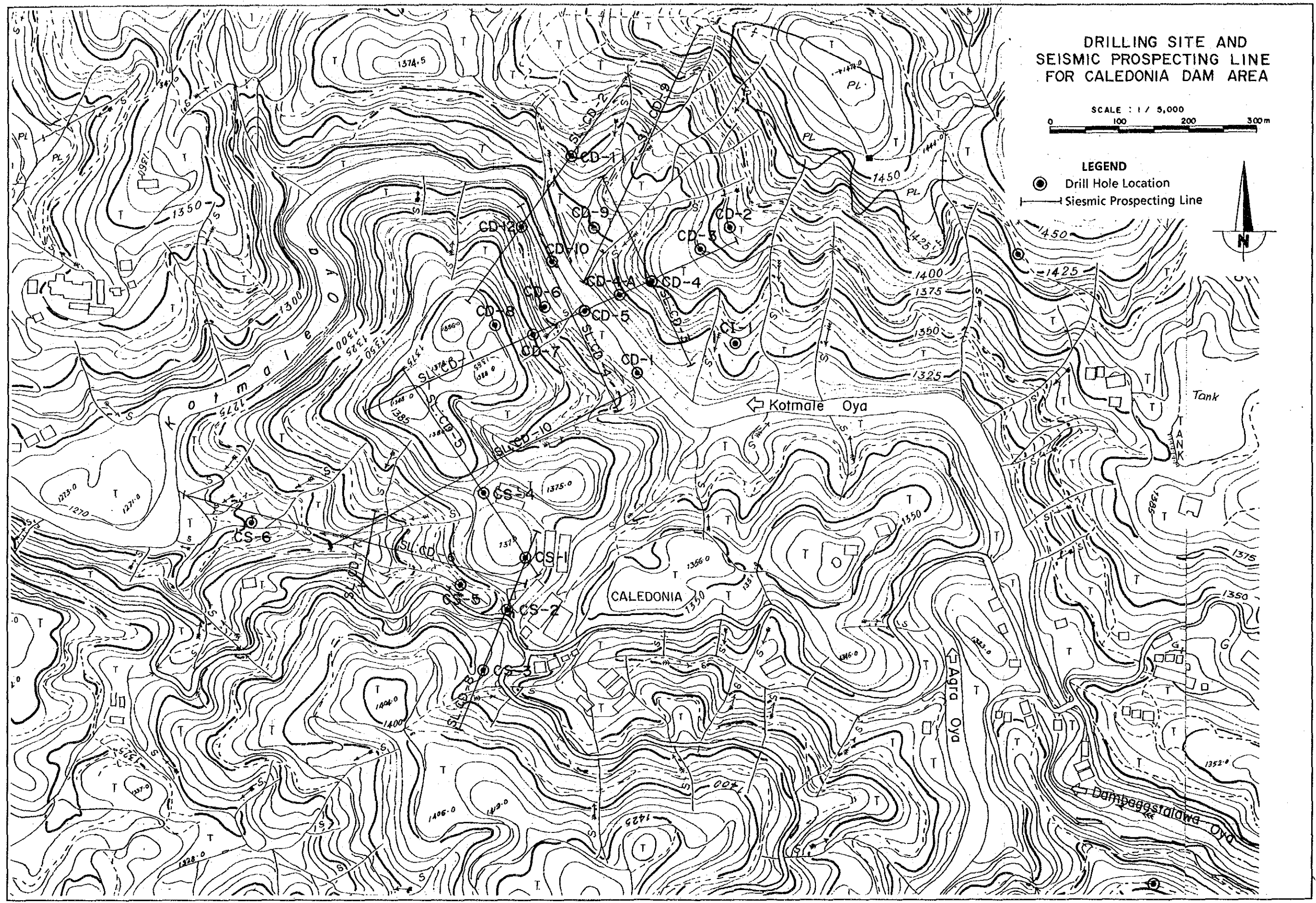
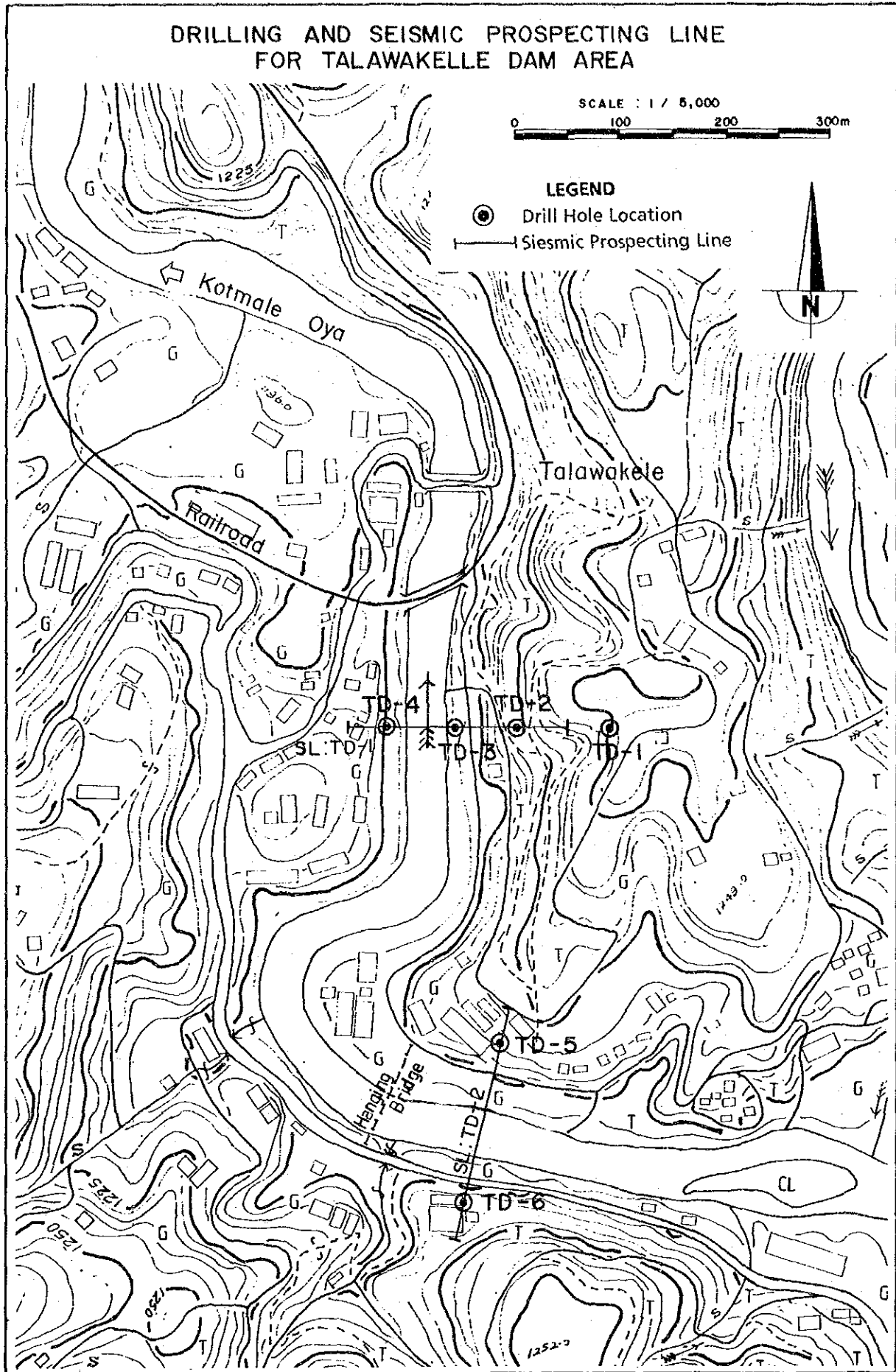


FIG. I. 2-2



DRILLING SITE AND SEISMIC PROSPECTING LINE FOR CALEDONIA P/S AREA

